UNITED NATIONS EDUCATIONAL, SCIENTIFIC AND CULTURAL ORGANIZATION
INTERNATIONAL ATOMIC ENERGY AGENCY
INTERNATIONAL CENTRE FOR THEORETICAL PHYSICS
I.C.T.P., P.O. BOX 586, 34100 TRIESTE, ITALY, CABLE: CENTRATOM TRIESTE

SMR.998b - 1

Research Workshop on Condensed Matter Physics
30 June - 22 August 1997
MINIWORKSHOP ON
SUPERCONDUCTING MESOSCOPIC STRUCTURES

14 - 25 JULY 1997

"Theory of Josephson effects in d-wave superconductors junctions"

Yukio TANAKA
Niigata University
Department of Physics
Faculty of Science
Ikarashi 2-Nocho
95021 Niigata
JAPAN

These are preliminary lecture notes, intended only for distribution to participants.

Theory of Josephson effects in d-wave superconductor junctions

Yukio TANAKA and Satoshi KASHIWAYA*

Department of Physics, Niigata University, Ikarashi, Niigata 950-21, Japan
**Electrotechnical Laboratory, Tsukuba, Ibaraki 305, Japan*

(Received May 25, 1997)

An analytical formula of the d.c. Josephson current in anisotropic superconductor junctions is presented. The formula is applicable for junctions with arbitrary insulating-potential height and thickness and with any symmetries including d-wave superconductors. In contrast to the formulas for conventional s-wave superconductors, the formula includes two additional effects. One is the intrinsic phase of the pair potential originating from the pairing symmetry in anisotropic superconductors. The other is the formation of localized states around the insulator. Using this formula, the Josephson current is calculated in s-wave superconductor / insulator / $d_{x^2-y^2}$-wave superconductor $(s/I/d)$, $d_{x^2-y^2}$-wave superconductor / insulator /$d_{x^2-y^2}$-wave superconductor $(d/I/d)$, $d_{x^2-y^2}$-wave superconductor / insulator / normal metal / insulator /$d_{x^2-y^2}$-wave superconductor $(d/I/n/I/d)$ junction configurations. In the case of $(d/I/d)$ and $(d/I/n/I/d)$ junction, the anomalous temperature dependence of the maximum Josephson current is calculated.

§1. Introduction

Recently, a growing amount of evidences have accumulated based on various theories and experimental data which point to the $d_{x^2-y^2}$ wave symmetry of the pair potentials[1]. In particular, the observations of anomalous magnetic field dependence in π-junctions[2)-4)] clearly verified that the pair potential in high-T_C superconductors encounter a phase change between a- and b-axis directions[5),6)]. Moreover, several other measurements using SQUIDs, Josephson junctions, or tricrystal rings[7)-10)], showed the results which are consistent with $d_{x^2-y^2}$-wave symmetry of the pair potentials. On the other hand, the properties of the Josephson junctions in d-wave superconductors have not been sufficiently revealed. At this stage, it is necessary to develop a new theory for the Josephson junctions in d-wave superconductors constructed on a microscopic basis.

A trial along this direction was done by one of us [Y.T.]. The d.c. Josephson current between s-wave superconductor /insulator/ $d_{x^2-y^2}$-wave superconductor $(s/I/d)$ junctions with $a(x)$, $b(y)$ and $c(z)$ axis orientations are calculated by taking into account the Andreev reflection[11)] and the normal reflection at the interface. This theory[12)] explains the anomalous magnetic field dependence of the maximum Josephson current $I_C(T)$ of the corner junction and corner SQUID[5),6)] naturally. In addition to this theory, several theories of Josephson junctions containing d-wave superconductors have been presented which take into account the anisotropy of the pair potential[13)-18)]. Although all of them have succeeded to reveal some aspects of the Josephson effect, one more essential effect, the existence of the zero energy states (ZES) around the insulator, has not been introduced yet.

The formation of surface bound states was originally discussed by Buchholtz and Zwicknagl[19] in p-wave superconductors. Hara and Nagai[20] investigated the ZES at the surface of p-wave polar states. Furthermore, the existence of zero energy bound states at the surface of d_{xy}-wave superconductors was obtained by Hu[21]. The properties of the zero-energy bound states and the local density of states of surface of d-wave superconductors were clarified recently in detail[22)-24]. On the other hand, the existence of zero-bias conductance peaks (ZBCP) at the surface of high-T_C superconductors was confirmed by several tunneling spectroscopy measurements[25)-28]. To reveal the line shape of the tunneling conductance, a novel tunneling theory was presented[29)-34] based on the quasiclassical approximations[35)-37]. It was revealed that the experimental ZBCP are closely related to the ZES[21] at the surface of d-wave superconductors. The theory which explains the various experimental line shapes of tunneling conductance[29),31),33] is completely distinct from that for an s-wave superconductor[38] in the sense that the tunneling spectroscopy is essentially sensitive to the phase of the pair potentials[31),33]. In Ref. 32, the physical origin of the ZES in several non-uniform superconductors are discussed in a unified way based on the quantum condition of the bound states of the quasiparticles. Similar effects can also be expected in Josephson junctions including d-wave superconductors[30] as the boundary effect around the insulator. In such situations, under the influence of the existence of ZES, the properties of the Josephson current in $s/I/d$ and $d/I/d$ junctions are expected to become anomalous[39)-42]. In this paper, we present an analytical formula for the d.c. Josephson current which fully takes into account the bound states around the insulator as well as the anisotropy of the pair potential. Although the self-consistency of the pair potential is neglected, the formula can be applicable to arbitrary barrier height and for spin singlet superconductors with any symmetry including d-wave and $s+id$-wave (time-reversed symmetry breaking case) superconductors. The obtained formula has a general form, and several existing theories can be derived from the formula as limiting cases[43)-48]. Using the formula, the Josephson current in $d/I/d$ and $s/I/d$ junctions are analyzed in detail. The organization of this paper is as follows. In § 2, a model for the Josephson current is given and the formula to calculate it is explicitly derived. The physical meaning of the formula is discussed in detail. In § 3, we clarify basic properties of $s/I/d$ junctions. In § 4, we address the basic properties of $d/I/d$ junctions. We calculate the grain angle dependence of the Josephson current. The validity of the theory by Sigrist and Rice (referred to as SR theory)[4] is discussed. In § 5, we discuss $d/I/n/I/d$ junctions. In § 6, we summarize our results.

§2. Model and Formulation

The Josephson current formula used in this study is essentially the extension of the previous formula for s-wave superconductors[45),46] to include the anisotropy of the pair potential. The formula is subsequently derived along with the original one.

The electron field operators $\Psi_\sigma(x_1,t)$ ($\sigma =\uparrow$ or $\downarrow$) satisfy the equation

$$i\hbar\frac{\partial}{\partial t}\Psi_\uparrow(x_1,t) = h_0\Psi_\uparrow(x_1,t) + \int dx_2\Delta(s,r)\Psi_\downarrow^\dagger(x_2,t), \qquad (2\cdot1)$$

$$i\hbar\frac{\partial}{\partial t}\Psi_\downarrow^\dagger(x_1,t) = -h_0\Psi_\downarrow^\dagger(x_1,t) + \int dx_2\Delta^*(s,r)\Psi_\uparrow(x_2,t). \qquad (2\cdot2)$$

with $s=(x_1-x_2)$, $r=(x_1+x_2)/2$, and $h_0=-\hbar^2\nabla_{x_1}^2/2m+U(x)-\mu$, where μ, $U(x)$, E, are the chemical potential, the Hartree potential, and the energy of a quasiparticle measured from the Fermi energy E_F ($E_F=\mu$). For the simplest model calculation, we consider a two-dimensional anisotropic singlet superconductor/ insulator /anisotropic singlet superconductor junction with perfectly flat interfaces in the clean limit. The system is assumed to be in the equilibrium state. In this model, the interface is perpendicular to the x-axis and is located at $x=0$ and $x=d_i$, where d_i is the magnitude of the thickness of the insulating region. The Fermi wave number k_F and the effective mass m are assumed to be equal both in the left and in the right side superconductors. The pair potential and Hartree potential are assumed to be

$$\Delta(k,r)=\begin{cases}\bar{\Delta}_L(\gamma)\exp(i\varphi_L), & x<0\\ 0, & 0<x<d_i\\ \bar{\Delta}_R(\gamma)\exp(i\varphi_R), & x>d_i\end{cases}\qquad U(x)=\begin{cases}0, & x<0\\ U_0, & 0<x<d_i\\ 0, & x>d_i,\end{cases} \qquad (2\cdot3)$$

where $\Delta(k,r)$ is the Fourier transform of $\Delta(s,r)$, with $\exp(i\gamma)\equiv k_x/\mid k\mid +ik_y/\mid k\mid$ using a wave vector k[35)-37)]. In the weak coupling limit, k is fixed on the Fermi surface ($\mid k\mid = k_F$). The quantities φ_L and φ_R are the macroscopic phases of the left and right superconductors, respectively. We will introduce a two-component Matsubara Green's function $G(x,x',i\omega_n)$, which are given as

$$G(x,x',i\omega_n)=\int_0^\beta G(x,x',\tau,\tau')\exp[i\omega_n(\tau-\tau')]d\tau, \qquad (2\cdot4)$$

$$G(x,x',\tau,\tau')=-\begin{pmatrix} <T_\tau\{\Psi_\uparrow(x,\tau)\Psi_\uparrow^\dagger(x',\tau')\}> & <T_\tau\{\Psi_\uparrow(x,\tau)\Psi_\downarrow(x',\tau')\}>\\ <T_\tau\{\Psi_\downarrow^\dagger(x,\tau)\Psi_\uparrow^\dagger(x',\tau')\}> & <T_\tau\{\Psi_\downarrow^\dagger(x,\tau)\Psi_\downarrow(x',\tau')\}>\end{pmatrix}. \qquad (2\cdot5)$$

Since the translational invariance is satisfied, the momentum parallel to the interface $k_y=k_F\sin\gamma$ is conserved. Taking this fact into account, the Green's function is transformed into a function k_y. From the conservation of the Josephson current for $E_{Fx}>>\mid\bar{\Delta}_L(\gamma)\mid,\mid\bar{\Delta}_R(\gamma)\mid$ with $E_{Fx}=\hbar^2k_F^2\cos^2\gamma/2m$, $I(\varphi)$ is reduced as

$$I(\varphi)=\frac{e\hbar k_BT}{2im}\lim_{x'\to x}\left(\frac{\partial}{\partial x'}-\frac{\partial}{\partial x}\right)\sum_{\omega_n,k_y}\mathrm{Tr}\{G(x,x',k_y,i\omega_n)\}\mid_{x=0}. \qquad (2\cdot6)$$

In the following, the Green's function is actually calculated in the junction configuration by extending the previous method[47)]. In this method, we assume four types of quasiparticle injection processes from both sides of the junction as the elementary processes as shown in Fig. 1 of Ref. 30. It is important to note that

the quasiparticles feel different pair potentials depending on the directions of their motions in anisotropic superconductors. For a given energy $E > (\max[\mid \tilde{\Delta}_R(\gamma_+) \mid, \mid \tilde{\Delta}_R(\gamma_-) \mid, \mid \tilde{\Delta}_L(\gamma_+) \mid, \mid \tilde{\Delta}_L(\gamma_-) \mid])$, with $\gamma_+ = \gamma$ and $\gamma_- = \pi - \gamma$, the wave functions $\Psi_l(x)$, $(l = 1 \cdots 4)$ corresponding to the four processes are expressed as

$$\Psi_l(x) = \exp(ik_F y \sin\gamma)\Psi_l(x,\gamma), \ (l = 1 \cdots 4) \tag{2·7}$$

$$\Psi_1(x,\gamma) = \begin{cases} \psi_{\alpha,L}(x,\gamma) + a_1\psi_{\bar{\alpha},L}(x,\gamma) + b_1\psi_{\beta,L}(x,\gamma), & (x < 0) \\ \psi_{1,I}(x,\gamma), & (0 < x < d_i) \\ g_1\psi_{\alpha,R}(x,\gamma) + h_1\psi_{\bar{\beta},R}(x,\gamma), & (x > d_i) \end{cases} \tag{2·8}$$

$$\Psi_2(x,\gamma) = \begin{cases} \psi_{\bar{\beta},L}(x,\gamma) + a_2\psi_{\beta,L}(x,\gamma) + b_2\psi_{\bar{\alpha},L}(x,\gamma), & (x < 0) \\ \psi_{2,I}(x,\gamma), & (0 < x < d_i) \\ g_2\psi_{\bar{\beta},R}(x,\gamma) + h_2\psi_{\alpha,R}(x,\gamma), & (x > d_i) \end{cases} \tag{2·9}$$

$$\Psi_3(x,\gamma) = \begin{cases} g_3\psi_{\beta,L}(x,\gamma) + h_3\psi_{\bar{\alpha},L}(x,\gamma), & (x < 0) \\ \psi_{3,I}(x,\gamma), & (0 < x < d_i) \\ \psi_{\beta,R}(x,\gamma) + a_3\psi_{\bar{\beta},R}(x,\gamma) + b_3\psi_{\alpha,R}(x,\gamma), & (x > d_i) \end{cases} \tag{2·10}$$

$$\Psi_4(x,\gamma) = \begin{cases} g_4\psi_{\bar{\alpha},L}(x,\gamma) + h_4\psi_{\beta,L}(x,\gamma), & (x < 0) \\ \psi_{4,I}(x,\gamma), & (0 < x < d_i) \\ \psi_{\bar{\alpha},R}(x,\gamma) + a_4\psi_{\alpha,R}(x,\gamma) + b_4\psi_{\bar{\beta},R}(x,\gamma), & (x > d_i) \end{cases} \tag{2·11}$$

where j expresses the indices L and R, and wave functions $\psi_{\alpha,j}(x,\gamma)$, $\psi_{\bar{\alpha},j}(x,\gamma)$ $\psi_{\beta,j}(x,\gamma)$ $\psi_{\bar{\beta},j}(x,\gamma)$ and $\psi_{l,I}(x,\gamma)$ are given as,

$$\psi_{\alpha,j}(x,\gamma) = \begin{pmatrix} u_j \exp(i\phi_j/2) \\ v_j \exp(-i\phi_j/2) \end{pmatrix} \exp[i(k_F\cos\gamma + \frac{m\Omega_{j,+}}{\hbar^2 k_F\cos\gamma})x], \tag{2·12}$$

$$\psi_{\bar{\alpha},j}(x,\gamma) = \begin{pmatrix} v_j \exp(i\phi_j/2) \\ u_j \exp(-i\phi_j/2) \end{pmatrix} \exp[i(k_F\cos\gamma - \frac{m\Omega_{j,+}}{\hbar^2 k_F\cos\gamma})x], \tag{2·13}$$

$$\psi_{\beta,j}(x,\gamma) = \begin{pmatrix} \tilde{u}_j \exp(i\tilde{\phi}_j/2) \\ \tilde{v}_j \exp(-i\tilde{\phi}_j/2) \end{pmatrix} \exp[-i(k_F\cos\gamma + \frac{m\Omega_{j,-}}{\hbar^2 k_F\cos\gamma})x], \tag{2·14}$$

$$\psi_{\bar{\beta},j}(x,\gamma) = \begin{pmatrix} \tilde{v}_j \exp(i\tilde{\phi}_j/2) \\ \tilde{u}_j \exp(-i\tilde{\phi}_j/2) \end{pmatrix} \exp[-i(k_F\cos\gamma - \frac{m\Omega_{j,-}}{\hbar^2 k_F\cos\gamma})x] \tag{2·15}$$

and

$$\psi_{l,I}(x,\gamma) = \begin{pmatrix} c_l\exp(-\lambda x) + d_l\exp(\lambda x) \\ e_l\exp(-\lambda x) + f_l\exp(\lambda x) \end{pmatrix}, \ (l = 1 \cdots 4), \tag{2·16}$$

with

$$u_j = \sqrt{\frac{1}{2}(1 + \frac{\Omega_{j,+}}{E})}, \ v_j = \sqrt{\frac{1}{2}(1 - \frac{\Omega_{j,+}}{E})}, \ \tilde{u}_j = \sqrt{\frac{1}{2}(1 + \frac{\Omega_{j,-}}{E})}, \ \tilde{v}_j = \sqrt{\frac{1}{2}(1 - \frac{\Omega_{j,-}}{E})}, \tag{2·17}$$

$$\Omega_{j,+} = \sqrt{E^2 - |\bar{\Delta}_j(\gamma_+)|^2},\ \Omega_{j,-} = \sqrt{E^2 - |\bar{\Delta}_j(\gamma_-)|^2},\ \lambda = \sqrt{\frac{2mU_0}{\hbar^2} - k_F^2\cos^2\gamma},$$

(2·18)

and

$$\exp(i\phi_j) = \frac{\bar{\Delta}_j(\gamma_+)}{|\bar{\Delta}_j(\gamma_+)|}\exp(i\varphi_j),\ \ \exp(i\tilde{\phi}_j) = \frac{\bar{\Delta}_j(\gamma_-)}{|\bar{\Delta}_j(\gamma_-)|}\exp(i\varphi_j). \qquad (2\cdot19)$$

Here, we have assumed the relation, $U_0, E_{Fx} >> |\Omega_{j,\pm}|$. The wave functions satisfy the following boundary conditions,

$$\Psi_l(x) = \begin{pmatrix} u_l(x) \\ v_l(x) \end{pmatrix},\ \Psi_l(x)|_{x=0_-} = \Psi_l(x)|_{x=0_+},\ \frac{d\Psi_l(x)}{dx}|_{x=0_-} = \frac{d\Psi_l(x)}{dx}|_{x=0_+}$$

(2·20)

$$\Psi_l(x)|_{x=d_{i,-}} = \Psi_l(x)|_{x=d_{i,+}},\ \frac{d\Psi_l(x)}{dx}|_{x=d_{i,-}} = \frac{d\Psi_l(x)}{dx}|_{x=d_{i,+}}. \qquad (2\cdot21)$$

From the conjugate processes of the above four wave functions, we obtain another set of wave functions $\hat{\Psi}_l(x)$ $(l = 1\cdots4)$ which satisfy

$$\int dx_1 \hat{\Psi}_l{}^t(x_1)\overleftarrow{H}(x_1, x_2) = E\hat{\Psi}_l{}^t(x_2),\ \ \hat{\Psi}_l(x_2) = \begin{pmatrix} \hat{u}(x_2) \\ \hat{v}(x_2), \end{pmatrix} \qquad (2\cdot22)$$

For an energy $E > (\max[|\bar{\Delta}_R(\gamma_+)|, |\bar{\Delta}_R(\gamma_-)|, |\bar{\Delta}_L(\gamma_+)|, |\bar{\Delta}_L(\gamma_-)|])$, $\hat{\Psi}_l(x)$ corresponds to the four elementary processes shown in Fig. 2 of Ref. 30. They also satisfy the boundary conditions given by Eqs. (2·20) and (2·21). As in the case of $\Psi_l(x)$, $\hat{\Psi}_l(x)$ can also be written as

$$\hat{\Psi}_l(x) = \exp(-ik_F y\sin\gamma)\hat{\Psi}_l(x,\gamma). \qquad (2\cdot23)$$

The explicit forms of these functions are not written here for brevity. Using the eight wave functions, Green's function is obtained as in Ref. 30. After an analytical continuation from E to $i\omega_n$, where $\omega_n = 2\pi k_B T(n + 1/2)$ denotes the Matsubara frequency, $\mathrm{Tr}\{G(x, x', k_y, i\omega_n)\}$ is obtained. By assuming $E_{Fx} >> |\bar{\Delta}_j(\theta_\pm)|$, $(j = L, R)$, the Josephson current $I(\varphi)$ is obtained as [41]

$$R_N I(\varphi) =$$

$$\frac{\pi\bar{R}_N k_B T}{e}\{\sum_{\omega_n}\int_{-\pi/2}^{\pi/2}[\frac{a_1(\theta, i\omega_n, \varphi)}{\Omega_{n,L,+}}|\bar{\Delta}_L(\theta_+)| - \frac{\tilde{a}_1(\theta, i\omega_n, \varphi)}{\Omega_{n,L,-}}|\bar{\Delta}_L(\theta_-)|]\cos\theta d\theta\},$$

(2·24)

where $\Omega_{n,L,\pm} = \mathrm{sgn}(\omega_n)\sqrt{\bar{\Delta}_L^2(\theta_\pm) + \omega_n^2}$. The quantity R_N denotes the normal resistance and $\bar{R}_N$ is expressed as

$$\bar{R}_N^{-1} = \int_{-\pi/2}^{\pi/2}\sigma_N\cos\theta d\theta,\ \ \sigma_N = \frac{4Z_\theta^2}{(1 - Z_\theta^2)^2\sinh^2(\lambda d_i) + 4Z_\theta^2\cosh^2(\lambda d_i)} \qquad (2\cdot25)$$

$$\lambda = (1 - \kappa^2\cos^2\theta)^{1/2}\lambda_0,\ \ Z_\theta = \frac{\kappa\cos\theta}{\sqrt{1 - \kappa^2\cos^2\theta}}, \qquad (2\cdot26)$$

where we have introduced two parameters $\lambda_0 = \sqrt{2mU_0/\hbar^2}$ and $\kappa = k_F/\lambda_0$. Here, σ_N denotes the tunneling conductance for the injected quasiparticle when the junction is in the normal state. In the above, $a_1(\theta, i\omega_n, \varphi)$ and $\tilde{a}_1(\theta, i\omega_n, \varphi)$ are given as

$$a_1(\theta, i\omega_n, \varphi) = i\frac{\Gamma_2(\theta, i\omega_n)\Gamma_5(\theta, i\omega_n)(1-\sigma_N) + \sigma_N\Gamma_6(\theta, i\omega_n, \varphi)\Gamma_3(\theta, i\omega_n, \varphi)}{\Gamma_1(\theta, i\omega_n)\Gamma_2(\theta, i\omega_n)(1-\sigma_N) + \sigma_N\Gamma_3(\theta, i\omega_n, \varphi)\Gamma_4(\theta, i\omega_n, \varphi)},$$

$$\tilde{a}_1(\theta, i\omega_n, \varphi) = i\frac{\Gamma_2(\theta, i\omega_n)\Gamma_7(\theta, i\omega_n)(1-\sigma_N) + \sigma_N\Gamma_8(\theta, i\omega_n, \varphi)\Gamma_4(\theta, i\omega_n, \varphi)}{\Gamma_1(\theta, i\omega_n)\Gamma_2(\theta, i\omega_n)(1-\sigma_N) + \sigma_N\Gamma_3(\theta, i\omega_n, \varphi)\Gamma_4(\theta, i\omega_n, \varphi)}, \quad (2\cdot27)$$

with (2·28)

$$\Gamma_1(\theta, i\omega_n) = 1 + \eta_{L,+}\eta_{L,-}, \Gamma_2(\theta, i\omega_n) = 1 + \eta_{R,+}\eta_{R,-}, \eta_{L(R),\pm} = \frac{\bar{\Delta}_{L(R)}(\theta_\pm)}{\omega_n + \Omega_{n,L(R),\pm}}. \quad (2\cdot29)$$

$$\Gamma_3(\theta, i\omega_n, \varphi) = 1 + \eta_{L,-}\eta_{R,-}\exp(-i\varphi), \Gamma_4(\theta, i\omega_n, \varphi) = 1 + \eta_{L,+}\eta_{R,+}\exp(i\varphi), \quad (2\cdot30)$$

$$\Gamma_5(\theta, i\omega_n) = \Gamma_{n,L,+} - \Gamma_{n,L,-}\exp[i(\alpha_+ - \alpha_-)], \quad (2\cdot31)$$

$$\Gamma_6(\theta, i\omega_n, \varphi) = \Gamma_{n,L,+} - \Gamma_{n,R,+}\exp[i(\varphi + \alpha_+ - \beta_+)], \quad (2\cdot32)$$

$$\Gamma_7(\theta, i\omega_n) = \Gamma_{n,L,-} - \Gamma_{n,L,+}\exp[i(\alpha_+ - \alpha_-)], \quad (2\cdot33)$$

$$\Gamma_8(\theta, i\omega_n, \varphi) = \Gamma_{n,L,-} - \Gamma_{n,R,-}\exp[i(-\varphi - \alpha_- + \beta_-)], \quad (2\cdot34)$$

$$\Gamma_{n,L,+} = \frac{\mathrm{sgn}(\omega_n) \mid \bar{\Delta}_L(\gamma_\pm) \mid}{\omega_n + \Omega_{n,L,\pm}}, \quad \Gamma_{n,R,+} = \frac{\mathrm{sgn}(\omega_n) \mid \bar{\Delta}_R(\gamma_\pm) \mid}{\omega_n + \Omega_{n,R,\pm}}, \quad (2\cdot35)$$

$$\Omega_{n,R,\pm} = \mathrm{sgn}(\omega_n)\sqrt{\bar{\Delta}_R^2(\theta_\pm) + \omega_n^2}, \quad (2\cdot36)$$

$$\exp(i\alpha_+) = \gamma_1, \ \exp(-i\alpha_-) = \gamma_2, \ \exp(-i\beta_+) = \gamma_3, \ \exp(i\beta_-) = \gamma_4. \quad (2\cdot37)$$

$$\gamma_1 = \frac{\bar{\Delta}_L(\theta_+)}{\mid \bar{\Delta}_L(\theta_+) \mid}, \ \gamma_2 = \frac{\mid \bar{\Delta}_L(\theta_-) \mid}{\bar{\Delta}_L(\theta_-)}, \ \gamma_3 = \frac{\mid \bar{\Delta}_R(\theta_+) \mid}{\bar{\Delta}_R(\theta_+)}, \ \gamma_4 = \frac{\bar{\Delta}_R(\theta_-)}{\mid \bar{\Delta}_R(\theta_-) \mid}. \quad (2\cdot38)$$

After straightforward calculations, we finally obtain the formula for the Josephson current as

$$R_N I(\varphi) = \frac{\pi\tilde{R}_N k_B T}{e}\{\sum_{\omega_n}\int_{-\pi/2}^{\pi/2}\tilde{F}(\theta, i\omega_n, \varphi)\sigma_N\cos\theta d\theta\}, \quad (2\cdot39)$$

$$\tilde{F}(\theta, i\omega_n, \varphi) = \frac{4\Gamma_{n,L,+}\Gamma_{n,R,+}(B_1 + B_2)}{\mid (1-\sigma_N)\Gamma_1(\theta, i\omega_n)\Gamma_2(\theta, i\omega_n) + \sigma_N\Gamma_3(\theta, i\omega_n, \varphi)\Gamma_4(\theta, i\omega_n, \varphi) \mid^2}, \quad (2\cdot40)$$

$$B_1 = (1-\sigma_N) \mid \Gamma_1(\theta, i\omega_n)\Gamma_2(\theta, i\omega_n) \mid \sin(\varphi + \alpha_+ - \beta_+ - \Psi_b) \quad (2\cdot41)$$

$$B_2 = \sigma_N \mid \Gamma_3(\theta, i\omega_n, \varphi) \mid^2 \sin(\varphi + \alpha_+ - \beta_+) \tag{2·42}$$

$$\exp(i\Psi_b) = \frac{\Gamma_1(\theta, i\omega_n)\Gamma_2(\theta, i\omega_n)}{\mid \Gamma_1(\theta, i\omega_n)\Gamma_2(\theta, i\omega_n) \mid}. \tag{2·43}$$

When the time reversal symmetry is not broken, $\bar{\Delta}_{L(R)}(\theta_\pm)$ is chosen as real quantities. Consequently, Eq. (2·39) can be simplified as [40),41)]

$$R_N I(\varphi) = \frac{\pi \bar{R}_N k_B T}{e} \{\sum_{\omega_n} \int_{-\pi/2}^{\pi/2} F(\theta, i\omega_n, \varphi) \sin\varphi \, \sigma_N \cos\theta d\theta\}, \tag{2·44}$$

$$F(\theta, i\omega_n, \varphi) = \frac{4\eta_{L,+}\eta_{R,+}[(1-\sigma_N)\Gamma_1(\theta, i\omega_n)\Gamma_2(\theta, i\omega_n) + \sigma_N \mid \Gamma_3(\theta, i\omega_n, \varphi) \mid^2]}{\mid (1-\sigma_N)\Gamma_1(\theta, i\omega_n)\Gamma_2(\theta, i\omega_n) + \sigma_N \Gamma_3(\theta, i\omega_n, \varphi)\Gamma_4(\theta, i\omega_n, \varphi) \mid^2}. \tag{2·45}$$

In the following, we will survey the intrinsic properties of the formulation [Eq. (2·39) and (2·44)]. Firstly, Eq. (2·39) can be applied to Josephson junctions whose electrodes have pairing symmetries which break time-reversal symmetry, *i.e.*, $\bar{\Delta}_{L(R)}(\theta_\pm)$ becomes complex. In general, $I(\varphi)$ can be decomposed into the series of $\sin(n\varphi)$ and $\cos(n\varphi)$

$$I(\varphi) = \sum_{n \geq 1} [I_n \sin(n\varphi) + J_n \cos(n\varphi)]. \tag{2·46}$$

When the time-reversal symmetry is not broken, J_n ($n \geq 1$) vanishes. Secondly, the formula includes the Josephson current component carried by the multiple reflection process at the interface. In the above equation, the current components with index n correspond to the amplitudes of the n-th reflection processes of quasiparticles. Thirdly, the formula naturally includes the bound states condition in the denominator of $\bar{F}(\theta, i\omega_n, \varphi)$ or $F(\theta, i\omega_n, \varphi)$, which we will refer to as $F_d(\theta, i\omega_n, \varphi)$. If we replace $i\omega_n$ with E, the condition $F_d(\theta, E, \varphi) = 0$ can be regarded as a linear combination of two types of bound-state conditions. For a high conductance junction ($\sigma_N \to 1$), the condition $F_d(\theta, E, \varphi) \approx \Gamma_3(\theta, E, \varphi)\Gamma_4(\theta, E, \varphi) = 0$ gives the energy levels of bound states formed between the diagonal pair potentials due to the Andreev-reflection process. For a low conductance junction ($\sigma_N \to 0$), the condition $F_d(\theta, E, \varphi) \approx \Gamma_1(\theta, E)\Gamma_2(\theta, E) = 0$ gives the energy levels of bound states formed around the surfaces of isolated semi-infinite superconductors. Fourthly, in Eq. (2·44), for a fixed φ, the direction of the current becomes either positive or negative depending on the angle. The sign of $F(\theta, i\omega_n, \varphi)$ is determined by the sign of numerator, *i.e.*, the sign of $\bar{\Delta}_R(\theta_+)\bar{\Delta}_L(\theta_+)$. The total Josephson current is regarded as the integration of all θ components. This is one of the important properties of the Josephson junction in anisotropic superconductors: the sign change of the pair potential on the Fermi surface.

Finally, Eqs. (2·39) and (2·44) are consistent with the previous formulae for the Josephson current as limiting cases. When the left and the right superconductors are s-wave superconductors with the same magnitude of the pair potential, we can choose $\bar{\Delta}_L(\theta_\pm) = \bar{\Delta}_R(\theta_\pm) = \Delta_0(T)$ and $\Omega_{n,L,\pm} = \Omega_{n,R,\pm} = \Omega_0 = \sqrt{\Delta_0^2(T) + \omega_n^2}$.

$\sqrt{\Delta_0^2(T)+\omega_n^2}$. The resulting $F(\theta, i\omega_n, \varphi)$ is expressed as

$$F(\theta, i\omega_n, \varphi) = \frac{4\Delta_0^2(T)}{4(1-\sigma_N)\Omega_0^2 + \sigma_N \mid (\omega_n+\Omega_0)+(\Omega_0-\omega_n)\exp(-i\varphi)\mid^2}. \quad (2\cdot47)$$

Performing the summation of the Matsubara frequency analytically, $R_N I(\varphi)$ is expressed as

$$R_N I(\varphi) = \frac{\pi \bar{R}_N}{e}\int_{-\pi/2}^{\pi/2} \frac{\Delta_0(T)\sigma_N \cos\theta \sin\varphi}{2\sqrt{1-\sigma_N \sin^2(\varphi/2)}} \tanh\left(\frac{\Delta_0(T)\sqrt{1-\sigma_N\sin^2(\varphi/2)}}{2k_BT}\right)d\theta. \quad (2\cdot48)$$

For $\sigma_N \sim 0$, $I(\varphi)$ is proportional to $\sin(\varphi)$ and the results by Ambegaokar and Baratoff's [AB] theory [48] is reproduced. While for $\sigma_N = 1$, Eq. (2·48) reproduces the previous results by Kulik and Ome'lyanchuk [43]. When the left and right superconductors are d-wave superconductors, four pair potentials are chosen as $\bar{\Delta}_L(\theta_\pm) = \Delta_d(T)\cos[2(\theta \mp \alpha)]$ and $\bar{\Delta}_R(\theta_\pm) = \Delta_d(T)\cos[2(\theta \mp \beta)]$. If we only take into account the $\theta = 0$ component of $F(\theta, i\omega_n, \varphi)$ in the θ integral of Eq. (2·44), we reproduce the Sigrist and Rice's [SR] theory [4] where $R_N I(\varphi)$ is proportional to $\cos(2\alpha)\cos(2\beta)$. When σ_N is set equal to unity, we can obtain the previous results by Yip [15] in pin-hole geometry. In the following sections, the Josephson junction in the various cases will be investigated in detail.

§3. Josephson effect in $s/I/d$ junction

In this section, the properties of the Josephson effect between s-wave superconductor and d-wave superconductor junctions are discussed. We consider a case when the ab-plane of the $d_{x^2-y^2}$-wave superconductor is in the plane as shown in Fig. 1A. The quantity β expresses the angle between the normal to the interface and the crystal axis (a-axis) of the $d_{x^2-y^2}$-wave superconductor. For a quasiparticle injection with angle θ to the interface normal, three effective pair potentials participate in this process. The most essential point is that the transmitted electron-like quasiparticle and hole-like quasiparticle do not always feel the same pair potentials. In such a situation, $\bar{\Delta}_L(\theta_\pm)$ and $\bar{\Delta}_R(\theta_\pm)$ are given as $\Delta_s(T)$ and $\Delta_d(T)\cos[2(\theta \mp \beta)]$, respectively. The quantities $\eta_{L,+}$ and $\eta_{L,-}$ in Eq. (2·29) are substituted with

$$\eta_{L,+} = \eta_{L,-} = \frac{\Delta_s(T)}{\omega_n + \Omega_{n,s}}, \Omega_{n,s} = \mathrm{sgn}(\omega_n)\sqrt{\omega_n^2+\Delta_s^2(\mathrm{T})}. \quad (3\cdot1)$$

To understand the current-phase relation $I(\varphi)$ clearly, the condition for the formation of ZES for $\sigma_N \to 0$ and the signs of $F(\theta, i\omega_n, \varphi)$ are summarized in Table 1 for $0 \le \beta \le \pi/4$. Although the particular choice of T_s and T_d is not essential, we select the critical temperatures of the s-wave superconductor and d-wave superconductor as T_s=8.8K $\sim$ 0.7meV/k_B and T_d=90 K $\sim$ 7.8meV/k_B, respectively. The corresponding $\Delta_s(0)$ and $\Delta_d(0)$ are 1.2meV and 18meV, respectively. Both $\Delta_s(T)$ and $\Delta_d(T)$ are assumed to obey the BCS relation. In Fig. 2, $I(\varphi)$ is plotted for various

β. Since the time reversal symmetry holds, $J_n = 0$ for $(n \geq 1)$ and $I(\varphi) = -I(-\varphi)$ is satisfied. At zero temperature, the quantity $F_d(\theta, 0, \varphi)$ vanishes for $\varphi = 0, \pm\pi$ for $\pm\pi/4 - \beta < \theta < \pm\pi/4 + \beta$. For non-zero β, ZES are formed at the interface and the resulting $I(\varphi)$ is also enhanced around $\varphi = 0$ and $\varphi = \pm\pi$ (curve a in Figs. 2B and 2C) at zero temperatures. When β is $\pi/4$ (Fig. 2C), I_1 vanishes and the contribution of I_2 becomes dominant. This is the reason for the period of oscillation of curves in Figs. 2C not being 2π but π. In this case, the Free energy minima is located at $\varphi = \pm\pi/2$ for $-\pi < \varphi < \pi$. The half periodic Josephson effect is also reported for s/n (normal metal)$/d$ junction [49),50)].

Figure 3 shows the temperature dependence of the maximum Josephson current $R_N I_C(T)$ for several cases. Without the barrier potential ($\sigma_N = 1$), the magnitude of $I_C(T)$ for $\beta = 0$ (curve a) is larger than the other cases independent of temperature (Fig. 3A). However, as σ_N decreases from one, *i.e.* as $\lambda_0 d_i$ increases, the magnitude of $I_C(T)$ for $\beta = \pi/4$ (curve c) enhances at low temperatures. For a low conductance junction ($\sigma_N \to 0$), if β deviates from zero, $\bar{\Delta}_R(\theta_+)\bar{\Delta}_R(\theta_-)$ becomes negative for $\pm\pi/4 - \beta < \theta < \pm\pi/4 + \beta$, and $F_d(\theta, i\omega_n, \varphi)$ is reduced at low temperatures. The extreme case is when $\beta = \pi/4$, where $\bar{\Delta}_R(\theta_+)\bar{\Delta}_R(\theta_-) < 0$ is satisfied for any θ. This is due to the formation of ZES at the interface. The reduction of $F_d(\theta, i\omega_n, \varphi)$ at low temperatures is much more drastic with the decrease of σ_N, *i.e.*, with the increase of $\lambda_0 d_i$. The resulting $I_C(T)$ is enhanced at low temperatures. Consequently, curves c in Figs. 3B and 3C have upper curvatures and are crucially different from those of AB theory [48)]. On the other hand, for $\beta = 0$ and $\sigma_N \to 0$, the temperature dependence of $I_C(T)$ is similar to those obtained by AB theory.

§4. Josephson effect in $d/I/d$ junction

This section presents the properties of d-wave superconductor / insulator /d-wave superconductor ($d/I/d$) Josephson junction. In the $d/I/d$ junction, for a quasiparticle injection from the left superconductor at an angle θ to the interface normal, four different effective pair potentials participate (Fig. 1B). The four effective pair potentials are $\bar{\Delta}_L(\theta_\pm) = \Delta_d(T)\cos[2(\theta \mp \alpha)]$ and $\bar{\Delta}_R(\theta_\pm) = \Delta_d(T)\cos[2(\theta \mp \beta)]$. The Josephson current is calculated by substituting the effective pair potentials to Eq. (2·29). The phenomenological theory by SR [4)] predicts that the maximum Josephson current is proportional to $|\cos(2\alpha)\cos(2\beta)|$. To clarify the validity of SR theory we define $J_C(\alpha, \beta, T) \equiv I_C(T)$ and introduce a function $B(\alpha, \beta, T)$ as

$$B(\alpha, \beta, T) = J_C(\alpha, \beta, T)/J_C(0, 0, T). \tag{4·1}$$

In SR theory, $B(\alpha, \beta, T)$ is proportional to $|\cos(2\alpha)\cos(2\beta)|$ for any temperatures. We now discuss the properties of $d/I/d$ junction and examine the validity of AB and SR theories for three types of geometry.

The temperature dependence of the maximum Josephson current $J_C(\alpha, \alpha, T)$ is plotted in Fig. 4. Since the quantity $F(\theta, i\omega_n, \varphi)$ is positive independent of θ, the maximum Josephson current $R_N J_C(\alpha, \alpha, T)$ is a monotonically increasing function with the decrease of temperatures. The enhancement of $J_C(\alpha, \alpha, T)$ with the decrease of temperature is most significant for $\alpha = \beta = \pi/4$. To understand these features,

it is instrumental to perform the summation of ω_n analytically which can be only possible for the special cases, $\alpha = \beta = 0$ and $\alpha = \beta = \pi/4$. For $\alpha = \beta = \pi/4$, where $\bar{\Delta}_{L(R)}(\theta_\pm) = \pm\bar{\Delta}_d(T,\theta) = \pm\Delta_d(T)\sin(2\theta)$ is satisfied, the resulting $R_N I(\varphi)$ becomes

$$R_N I(\varphi) = \frac{\pi\bar{R}_N}{e}\int_{-\pi/2}^{\pi/2}\frac{\bar{\Delta}_d(T,\theta)\sigma_N\cos\theta\sin\varphi}{2\sqrt{\sigma_N}\cos(\varphi/2)}\tanh[\frac{\bar{\Delta}_d(T,\theta)\cos(\varphi/2)\sqrt{\sigma_N}}{2k_BT}]d\theta,$$

and for $\sqrt{\sigma_N}\mid\bar{\Delta}_d(T,\theta)\mid << 2k_BT$, (4·2)

$$R_N J_C(\pi/4,\pi/4,T) = \frac{\pi\bar{R}_N}{4ek_BT}\int_{-\pi/2}^{\pi/2}\bar{\Delta}_d^2(T,\theta)\sigma_N d\theta. \tag{4·3}$$

Since the temperature is included in the denominator, the Josephson current is expected to increase as the temperature is lowered. This anomalous behavior originates from the existence of ZES at the interfaces of both the left and the right superconductors (curves c in Fig. 4 A and B). At sufficiently low temperatures, *i.e.*, $k_BT << \sqrt{\sigma_N}\mid\bar{\Delta}_d(T,\theta)\mid$, $R_N J_C(\pi/4,\pi/4,T)$ is given as

$$R_N J_C(\pi/4,\pi/4,T) \sim \frac{\pi\bar{R}_N}{e}\int_{-\pi/2}^{\pi/2}\mid\bar{\Delta}_d(T,\theta)\mid\sqrt{\sigma_N}\cos\theta d\theta. \tag{4·4}$$

Since the order of the magnitude of $\bar{R}_N$ is proportional to the inverse of σ_N, at low temperatures, $R_N J_C(\pi/4,\pi/4,T)$ is proportional to the inverse of $\sqrt{\sigma_N}$[40),51)]. Hence we can expect large magnitude of $R_N J_C(\pi/4,\pi/4,T)$ for a low conductance junction with $\alpha = \beta = \pi/4$. Figure 5 shows the calculated results of the $B(\alpha,\alpha,T)$ as a function of α for various temperatures. Curves a to c show that $B(\alpha,\alpha,T)$ takes the maximum value at $\alpha = \pi/4$ in low temperature region. As the temperature is lowered and as $\lambda_0 d_i$ is increased, the magnitude of $B(\pi/4,\pi/4,T)$ is enhanced. This anomalous α dependence can not be explained in the framework of SR theory (curve *d*). Let us discuss the Josephson current originating from the region C where ZES are formed for small σ_N. The quantity $I_z(\varphi)$ is given as

$$R_N I_z(\varphi) = \frac{\pi\bar{R}_N}{e}k_BT\sum_{\omega_n}H(i\omega_n)\sin(\varphi),\quad H(i\omega_n) = \int_C F(\theta,i\omega_n,\varphi)\sigma_N\cos\theta d\theta. \tag{4·5}$$

For sufficiently low temperature with small σ_N, *i.e.*, $\sqrt{\sigma_N}\mid\bar{\Delta}_d(T,\theta)\mid << \omega_n$, $H(i\omega_n)$ becomes

$$H(i\omega_n) = 8\int_{\pi/4-\alpha}^{\pi/4+\alpha}\frac{\sigma_N\cos\theta\mid\bar{\Delta}_L(\theta_+)\mid^2\mid\bar{\Delta}_L(\theta_-)\mid^2}{\omega_n^2[\mid\bar{\Delta}_L(\theta_+)\mid+\mid\bar{\Delta}_L(\theta_-)\mid]^2}d\theta \propto \omega_n^{-2}, \tag{4·6}$$

with $\bar{\Delta}_L(\theta_\pm) = \bar{\Delta}_R(\theta_\pm)$, and the resulting $R_N I_C(T)$ is proportional to the inverse of T. This anomalous ω_n dependence of $H(i\omega_n)$ is the origin of the deviation from that of SR theory.

Secondly, we assume a mirror type junction ($\alpha = -\beta$). The quantity $F(\theta,i\omega_n,\varphi)$ becomes negative (positive) for $\pm\pi/4 - \alpha < \theta < \pm\pi/4 + \alpha$ with $0 < \varphi < \pi$ ($-\pi <$

$\varphi < 0$). These conditions happen to coincide with those of the formation of ZES both at the left and right interfaces. Typical $I(\varphi)$ and $R_N J_C(\alpha, -\alpha, T)$ are shown in Figs. 6 and 7, respectively. When $\lambda_0 d_i = 0$, the magnitude of $I(\varphi)$ increases with the decrease in temperatures (Fig.6A and curves a in Fig. 7). But when $\lambda_0 d_i$ becomes non-zero, the magnitudes of $I(\varphi)$ and $J_C(\alpha, -\alpha, T)$ show non-monotonous behavior with temperature (Fig. 6B and curves b, c, in Fig. 7A). As α increases, $I(\varphi)$ changes sign with decrease in T for fixed φ (Figs. 6C and 6D). The magnitude of $J_C(\alpha, -\alpha, T)$ has anomalous temperature dependence as shown in curves b and c in Figs. 7B and C. In this case, $H(i\omega_n)$ for small magnitude of ω_n and $\sqrt{\sigma_N} \mid \bar{\Delta}_d(T, \theta) \mid << \omega_n$ is expressed as

$$H(i\omega_n) = -8 \int_{\pi/4-\alpha}^{\pi/4+\alpha} \frac{\sigma_N \cos\theta \mid \bar{\Delta}_L(\theta_+) \mid^2 \mid \bar{\Delta}_L(\theta_-) \mid^2}{\omega_n^2 [\mid \bar{\Delta}_L(\theta_+) \mid + \mid \bar{\Delta}_L(\theta_-) \mid]^2} d\theta \propto \omega_n^{-2}, \tag{4·7}$$

with $\bar{\Delta}_L(\theta_\pm) = \bar{\Delta}_R(\theta_\mp)$. This anomalous ω_n dependence is similar to the case of $\alpha = \beta$ and induces the non-monotonous temperature dependencies of $J_C(\alpha, -\alpha, T)$. To understand this effect clearly, three parameters $G_p(\varphi)$, $G_n(\varphi)$ and φ_M are defined. Since the sign of $R_N I(\varphi)$ has φ-dependence, $R_N I(\varphi)$ is decomposed into a negative component $G_n(\varphi)$ and a positive component $G_p(\varphi)$. When $0 < \varphi < \pi$, they are expressed as

$$G_n(\varphi) = \frac{\bar{R}_N \pi k_B T}{e} \times \{\sum_{\omega_n} \int_{-\pi/4-\alpha}^{-\pi/4+\alpha} F(\theta, i\omega_n, \varphi) \sigma_N \cos\theta d\theta + \int_{\pi/4-\alpha}^{\pi/4+\alpha} F(\theta, i\omega_n, \varphi) \sigma_N \cos\theta d\theta\} \sin\varphi, \tag{4·8}$$

and $G_p(\varphi) = R_N I(\varphi) - G_n(\varphi)$. On the other hand, when $-\pi < \varphi < 0$, they are given by

$$G_p(\varphi) = \frac{\bar{R}_N \pi k_B T}{e} \times \{\sum_{\omega_n} \int_{-\pi/4-\alpha}^{-\pi/4+\alpha} F(\theta, i\omega_n, \varphi) \sigma_N \cos\theta d\theta + \int_{\pi/4-\alpha}^{\pi/4+\alpha} F(\theta, i\omega_n, \varphi) \sigma_N \cos\theta d\theta\} \sin\varphi, \tag{4·9}$$

and $G_n(\varphi) = R_N I(\varphi) - G_p(\varphi)$. The quantity φ_M ($-\pi < \varphi_M < \pi$) is defined as the phase difference giving the maximum amplitude of $I(\varphi)$. In Fig. 8, $\mid G_n(\varphi_M) \mid$ and $G_p(\varphi_M)$ are plotted using the same parameters as curve b in Fig. 7B. With the increase in α, the jump of φ_M occurs as shown in Fig. 8 (see inset of Fig. 8). Near the temperature of the jump, $T \sim T_j$, the shape of $I(\varphi)$ changes as shown in Fig. 9. The non-monotonous temperature dependence and the enhancement of $R_N J_C(\alpha, -\alpha, T)$ below T_j originate from the jump of φ_M from positive to negative and from the enhancement of $G_p(\varphi_M)$ with negative φ_M. With the further increase of α, φ_M stays negative independent of temperature. In this case, $R_N J_C(\alpha, -\alpha, T)$ becomes a monotonically increasing function with the decrease of temperatures since $G_p(\varphi_M) > \mid G_n(\varphi_M) \mid$ is satisfied for all temperatures. The comparison of our results with that of SR theory for a fixed temperature is plotted in Fig. 10. There is a

double minima in $B(\alpha, -\alpha, T)$. The width of the peak at $\alpha = \pi/4$ increases as the temperature is decreased. The height of the peak enhances with the increase of the magnitude of $\lambda_0 d_i$. These features are remarkably different from those expected from SR theory (curve d).

Finally, the applicability of AB and SR theories is summarized. Both theories assume junctions with low conductance and ignore the existence of the ZES. We can apply AB theory only when there is no ZES for every θ at the interface, *i.e.*, $\alpha = \beta = 0$ is satisfied. In SR theory, only the current component which flows perpendicular to the interface is considered. In the case when one of the interfaces of the superconductor has no ZES for every θ, *i.e.*, $\alpha = 0$ ($\beta = 0$) is satisfied, the β (α) dependence of the maximum Josephson current is expressed by SR theory fairly well. However, when both superconductors have ZES, *e.g.* for $\alpha = \beta$ or $\alpha = -\beta$, large deviation exists from SR theory [4]. The mid gap states influence significantly on the flux quantization in tricrystal rings [39),52)].

§5. Josephson effect in $d/I/n/I/d$ junction

Following a similar method as in §2, the Josephson current through $d/I/n/I/d$ junction is formulated from the coefficient of the Andreev reflection of a quasiparticle injected from the left superconductor [53]. The flat interfaces are simply expressed as δ-function model with the amplitude of H and are located at $x = 0$ and $x = L$. We will define the coherence length of the superconductor which are given as $\xi = \hbar v_F/\Delta(T)$, where v_F is the magnitude of the Fermi velocity in the normal metal. For the barrier height parameter, a dimensionless variable Z_0 which are given as $Z_0 = 2mH/(\hbar^2 \mid k_F \mid)$ is used. The Josephson current is explicitly given as

$$R_N I(\varphi) = \frac{\pi \tilde{R}_N k_B T}{e} \{ \sum_{\omega_n} \int_{-\pi/2}^{\pi/2} F(\theta, i\omega_n, \varphi) \sin\varphi \sigma_N \cos\theta d\theta \} \tag{5·1}$$

$$F(\theta, i\omega_n, \varphi) = \frac{4\gamma\eta_{R,+}\eta_{L,+}\sigma_N \{(1-\sigma_N)CDt + [\mid A_- \mid^2 - (1-\sigma_N)\gamma^2 \mid B_- \mid^2]\sigma_N\}}{\mid \sigma_N[A_+A_- - \gamma^2(1-\sigma_N)B_+B_-] + (1-\sigma_N)CDt \mid^2} \tag{5·2}$$

$$A_\pm = 1 + \gamma\eta_{R,+}\eta_{L,+}\exp(\pm i\varphi), B_\pm = 1 + \frac{1}{\gamma}\eta_{R,+}\eta_{L,+}\exp(\pm i\varphi), \tag{5·3}$$

$$C = 1 + \eta_{R,+}\eta_{R,-}, D = 1 + \eta_{L,+}\eta_{L,-} \tag{5·4}$$

$$\eta_{R(L),\pm} = \frac{\Delta_{R(L),\pm}(\theta)}{\Omega_{n,R(L),\pm} + \omega_n}, \ \Omega_{n,R(L),\pm} = \sqrt{\Delta^2_{R(L),\pm}(\theta) + \omega_n^2}, \tag{5·5}$$

$$\gamma = \exp[-\frac{2m \mid \omega_n \mid L}{\hbar^2 q_{Fx}}], t = (1 - \gamma t_s\delta)(1 - \frac{\gamma}{t_s\delta}), t_s = \frac{(t_r + 1 - iZ)(t_r - 1 - iZ)}{(t_r + 1 + iZ)(t_r - 1 + iZ)}, \tag{5·6}$$

$$\bar{R}_N = \int_{-\pi/2}^{\pi/2} \sigma_N \cos\theta d\theta \tag{5·7}$$

$$\sigma_N = \frac{4t_r}{[(1+t_r)^2+Z^2]},\ Z = \frac{Z_0}{\cos\theta},\ t_r = \frac{q_{Fx}}{k_{Fx}},\ \delta = \exp(2iq_{Fx}L) \tag{5·8}$$

The quantity φ denotes the macroscopic phase difference between two superconductors. In the above, $k_{Fx} = k_F \cos\theta$ and q_{Fx} is the x component of the Fermi momentum in the superconductor and the normal metal. The quantity θ denotes the injection angle of the quasiparticles as in §2 – §4. The spherical Fermi surfaces in both of the normal metal and the superconductor are assumed. The magnitude of the Fermi momentum in the superconductor k_F is equal to or smaller than that of in the normal metal q_F. The available Fermi surface in the normal metal is restricted for $q_F > k_F$. The effective pair potentials are given as a function of θ. For d-wave symmetry, they are given as

$$\Delta_{L,\pm}(\theta) = \Delta(T)\cos[2(\theta \mp \alpha)],\ \Delta_{R,\pm}(\theta) = \Delta(T)\cos[2(\theta \mp \beta)], \tag{5·9}$$

where α and β expresses the angle between the crystal axis and the normal to the interface as in Fig. 1. In the case, both left and right superconductors are replaced with s-wave superconductors, we reproduce several previous results [43)-46), 48)].

Since we are now interested in the regime where $q_{Fx}L >> 1$ is satisfied, it is more realistic to average out the rapidly oscillating factors. The averaged out Josephson current is obtained as

$$R_N\bar{I}(\varphi) = \frac{1}{2\pi}\int_0^{2\pi} R_N I(\varphi)d\theta,\quad \theta = 2q_{Fx}L + Arg(t_s) \tag{5·10}$$

In the following calculation, we will assume $k_F = q_F$ and $Z_0 = 5$. In Fig. 11, temperature dependence of the maximum Josephson current is plotted for $\alpha = \beta = 0$. The obtained results are drastically different from those based on Ambegaokar and Baratoff's theory [48)]. Here T_d is a critical temperature of d-wave superconductor. The non-monotonous temperature dependence appears for $\alpha = -\beta$ as shown in Fig. 12. With the increase of L, the non-monotonous behavior is rapidly suppressed. The results show that the current depends on the width of the normal metal, the magnitude of the insulating barrier, and crystal orientation. Similar to the case of the $d/I/d$ junction, non-monotonous temperature dependence of the Josephson current is predicted. The role of the ZES is suppressed for long normal metal [54)].

§6. Summary and discussion

An analytical formula for the d.c. Josephson current in spin-singlet anisotropic superconductors has been presented. We have taken into account the fact that quasiparticles feel the different signs of the pair potentials depending on the directions of their motions [40)-42)]. Our novel formula is general in the sense that several existing formula for the Josephson current can be derived as limiting cases [15), 43)-46), 48)].

This formula is valid, even when the time reversal symmetry is broken, *i.e.*, the pair potential of the superconductor becomes a complex number. Since the multiple Andreev reflection and the normal reflection at the interface are completely included, the formula can be applicable for arbitrary barrier height case.

Applying our novel formula, the Josephson current is calculated for various types of the junction geometry. The calculated results show several anomalous behaviors which are not expected for Josephson junctions of conventional s-wave superconductors. Especially, three important features are predicted for Josephson junctions including d-wave superconductors:

1. For a fixed phase difference between two superconductors, the component of the Josephson current becomes either positive or negative depending on the injection angle of the quasiparticle.
2. In some situations, the phase difference φ_0, which gives the free energy minima, is located at neither zero nor π.
3. When the crystal axis is tilted from the interface normal, zero-energy states (ZES), *i.e.*, mid gap states are formed near the interface depending on the angle of the crystal axis and the injection angle of the quasiparticle. The existence of ZES enhances the Josephson current at low temperatures.

These features will be confirmed if they will actually be measured in the experiments. Throughout this paper, the spatial dependence of the pair potentials are assumed to be constant. Even if the depletion of the pair potentials around the interface is taken into account, the ZES does not vanish at all[24], and the essential results will not be changed. Recently, Barash, Burkhardt and Rainer calculated the Josephson current in grain boundary $d/I/d$ junction[55)-57)]. Their theory includes the effect of roughness and the self-consistency of the spatial dependence of the pair potential. The qualitative features of Josephson current, *i.e.*, a non-monotonous temperature dependence of the Josephson current, anomalous phase dependence, are not changed at all when the effect of the roughness is small. There is a possibility of coexistence of s-wave pairing[58),59)] near the interface. This effect is important in the underdoped region, *i.e.* near the Mott transition, where the effective attractive potential is strong[60)]. It is an interesting problem to clarify the role of induced s-wave component on the d.c. Josephson current. In this paper, only the Josephson current with zero voltage is discussed. Very recently, Barash and Svidzinsky[57)] investigated the singular behavior of the quasiparticle current and the Josephson current for non-zero voltage in $d/I/d$ junction in the limit of low transparency coefficient. To clarify the Josephson current and the quasiparticle current[61)] for arbitrary transparency.[62)] is also a challenging future problem.

References

1) D.J. Scalapino, Phys. Rep. 250, 329 (1995).
2) V.B. Geshkenbein, A.I. Larkin, and A. Barone, Phys. Rev. B 36, 235 (1987).
3) L.N. Bulaevskii, V.V. Kuzii, and A.A. Sobyanin, JETP Lett. 25, 290 (1977).
4) M. Sigrist and T.M. Rice, J. Phys. Soc. Jpn. 61, 4283 (1992); Rev. Mod. Phys. 67, 503

(1995).
5) D. A. Wollman, D.J. van Harlingen, W. C. Lee, D. M. Ginsberg, and A.J. Leggett, Phys. Rev. Lett. 71, 2134 (1993).
6) D. J. Van Harlingen, Rev. Mod. Phys. 67, 515 (1995).
7) I. Iguchi and Z. Wen, Phys. Rev. B 49, 12388 (1994).
8) J.R. Kirtley, C.C. Tsuei, M. Rupp, J.Z. Sun, Lock See Yu-Jahnes, A. Gupta, and M.B. Ketchen, Phys. Rev. Lett. 76, 1336 (1996).
9) D.A. Brawner and H.R. Ott, Phys. Rev. B 50, 6530 (1994).
10) A. Barone, Nuovo Cimento 16D, 1635 (1994).
11) A. F. Andreev Zh. Eksp. Teor. Fiz. 46, 1823 (1964). [Sov. Phys.-JETP 19, 1228 (1964)].
12) Y. Tanaka, Phys. Rev. Lett. 72, 3871 (1994), Physica C 235-240, 3205 (1994).
13) S. Yip, J. Low. Temp. Phys. 91, 203 (1993).
14) Yu.S. Barash, A.V. Galaktionov, and A.D. Zaikin, Phys. Rev. B 52, 665 (1995).
15) S. Yip, Phys. Rev. B 52, 3087 (1995).
16) C. Bruder, A. van Otterlo, and G.T. Zimanyi, Phys. Rev. B 51, 12904 (1994).
17) Weiyi Zhang, Phys. Rev. B 52, 3772 (1995); 52, 12538 (1995).
18) G. Deutscher and R. Maynard, Europhys. Lett. 30, 361 (1995).
19) L.J. Buchholtz and G. Zwicknagl, Phys. Rev. B B23, 5788 (1981).
20) J. Hara and K. Nagai, Prog. Theor, Phys. 74, 3451 (1986).
21) C.R. Hu, Phys. Rev. Lett. 72, 1526 (1994).
22) Jian Yang and C.R. Hu, Phys. Rev. B 50, 16766 (1994).
23) M. Matsumoto and H. Shiba, J. Phys. Soc. Jpn. 64, 1703 (1995).
24) Y. Nagato and K. Nagai, Phys. Rev. B 51, 16254 (1995).
25) J. Geerk, X.X. Xi, and G. Linker, Z. Phys. B 73, 329 (1988).
26) I. Iguchi, Physica C 185-189, 241 (1991).
27) S. Kashiwaya, M. Koyanagi, M. Matsuda, and K. Kajimura, Physica B 194-196, 2119 (1994).
28) L. Alff, H. Takashima, S. Kashiwaya, N. Terada, H. Ihara, Y. Tanaka, M. Koyanagi and K. Kajimura, Phys. Rev. B, 55, (1997).
29) S. Kashiwaya, Y. Tanaka, H. Takashima, Y. Koyanagi, and K. Kajimura, Phys. Rev. B 51, 1350 (1995).
30) Y. Tanaka and S. Kashiwaya, Phys. Rev. B 53, 9371 (1996).
31) Y. Tanaka and S. Kashiwaya, Phys. Rev. Lett. 74, 3451 (1995).
32) S. Kashiwaya, Y. Tanaka, M. Koyanagi, and K. Kajimura, *Advances in Superconductivity VII*, ed. K.Yamafuji and T. Morishita (Springer-Verlag Tokyo 1995) 45; Jap. J. Appl. Phys. 34, 4555 (1995).
33) S. Kashiwaya, Y. Tanaka, M. Koyanagi, and K. Kajimura, Phys. Rev. B, 53, 2667 (1996); J. Phys. Chem. Solid, 56, 1721 (1995).
34) Yu.S. Barash, A.V. Svidzinsky and H. Burkhardt, prepint, [condmat9705018].
35) C. Bruder, Phys. Rev. B 41, 4017 (1990).
36) A. Millis, D. Rainer, and J.A. Sauls, Phys. Rev. B 38, 4504 (1988).
37) J. Kurkijärvi and D. Rainer, in *Modern Problems in Condensed Matter Sciences*, edited by W.P. Halperin and L.P. Pitaevskii (Elsevier, Amsterdam, 1989).
38) G.E. Blonder, M. Tinkham, and T.M. Klapwijk, Phys. Rev. B 25, 4515 (1982).
39) Y. Tanaka and S. Kashiwaya, *Advances in Superconductivity VIII*, ed. H. Hayakawa and Y. Enomoto (Springer-Verlag Tokyo 1996) 259.
40) Y. Tanaka and S. Kashiwaya, Phys. Rev. B 56, (1997).
41) Y. Tanaka and S. Kashiwaya, J. Phys. Chem. Solids 56, 1761 (1995); Phys. Rev. B 53, R11957 (1996).
42) Y. Tanaka, S. Kashiwaya, M. Koyanagi, and K. Kajimura, Physica C 262, 238 (1996).
43) I.O. Kulik and A.N. Omelyanchuk, Fiz. Nizk. Temp. 4, 296 (1978), [Sov. J. Low Temp. Phys. 4, 142 (1978)].
44) C. Ishii, Prog. Theor. Phys. 44, 1525 (1970); 47, 1464 (1972).
45) A. Furusaki and M. Tsukada, Solid State Commun. 78, 299 (1991).
46) G.B. Arnold, J. Low Temp. Phys. 59, 143 (1985).
47) W. L. McMillan, Phys. Rev. B 175, 559 (1967).
48) V. Ambegaokar and A. Baratoff, Phys. Rev. Lett. 10, 486 (1963).
49) A. Huck, A. van Otterlo, and M. Sigrist, preprint, [condmat9705025].

50) A.M. Zagoskin, preprint, [condmat9702123v2].
51) R.A. Riedel and P.F. Bagwell, unpublished.
52) M.P. Samanta and S. Datta, Phys. Rev. B, 55, R8689, (1997).
53) Y. Tanaka and S. Kashiwaya, to be published in Physica C.
54) S. Datta, M. Samanta, preprint, [condmat9606065].
55) Yu. S. Barash, H. Burkhardt, and D. Rainer, Phys. Rev. Lett. 77, 4070 (1996).
56) H. Burkhardt, to be published in it Quasiclassical Theory of Superconductivity in Strongly Correlated Systems, editied by D. Rainer and J.A. Sauls (Springer-Verlag, 1997).
57) Yu. S Barash and A.A. Svidzinsky, to be published in it Quasiclassical Theory of Superconductivity in Strongly Correlated Systems, editied by D. Rainer and J.A. Sauls (Springer-Verlag, 1997); Zh. Eksp. Teor. Fiz. 111, 1 (1997).
58) M. Matsumoto and H. Shiba, J. Phys. Soc. Jpn. 64, 3384 (1995); 64, 4867 (1995); 65, 2194 (1996).
59) L.J. Buchholtz, M. Palumbo, D. Rainer, and J.A. Sauls, J. Low Temp. Phys. 101, 1079 (1995); 101, 1097 (1995).
60) M. Ogata, unpublished.
61) S. Kashiwaya, Y. Tanaka, M. Koyanagi, S. Ueno, and K. Kajimura, to be published in Physica C.
62) M. Hurd, preprint, [condmat9702028].

Captions for Figures

Fig. 1. Schematic illustration of reflection and transmission of quasiparticles at the interface. A: s-wave superconductor / insulator $/d_{x^2-y^2}$-wave superconductor $(s/I/d)$ junction. B: $d_{x^2-y^2}$-wave superconductor / insulator $/d_{x^2-y^2}$-wave superconductor $(d/I/d)$ junction.

Fig. 2. Josephson current $I(\varphi)$ plotted as a function of φ for $\lambda_0 d_i = 1$ and $\kappa = 0.5$ with A: $\beta = 0$, B: $\beta = \pi/8$, and C: $\beta = \pi/4$. a: $T/T_s = 0.05$, b: $T/T_s = 0.3$, and c: $T/T_s = 0.6$.

Fig. 3. Maximum Josephson current $I_C(T)$ plotted as a function of temperature for $\kappa = 0.5$. A: $\lambda_0 d_i = 0$, B: $\lambda_0 d_i = 0.5$, and C: $\lambda_0 d_i = 1$. a: $\beta = 0$, b: $\beta = \pi/8$, and c: $\beta = \pi/4$.

Fig. 4 Maximum Josephson current $J_C(\alpha, \beta, T)$ in $d/I/d$ junction with $\alpha = \beta$ plotted as a function of temperature with $\kappa = 0.5$. A: $\lambda_0 d_i = 1$ and B: $\lambda_0 d_i = 3$. a: $\alpha = 0$, b: $\alpha = \pi/8$, and c: $\alpha = \pi/4$.

Fig. 5. $B(\alpha, \alpha, T)$ plotted as a function of α for A: $\lambda_0 d_i = 1$ and B: $\lambda_0 d_i = 3$ with $\kappa = 0.5$. a: $T/T_d = 0.05$, b: $T/T_d = 0.3$, c: $T/T_d = 0.6$, and d: Sigrist and Rice's result (SR theory).

Fig. 6. Josephson current $I(\varphi)$ in $d/I/d$ junction plotted as a function of φ for $\kappa = 0.5$ and $\alpha = -\beta$. A: $\alpha = 0.05\pi$, $\lambda_0 d_i = 0$, B: $\alpha = 0.05\pi$, $\lambda_0 d_i = 2$, C: $\alpha = 0.1\pi$, $\lambda_0 d_i = 2$, and D: $\alpha = 0.12\pi$, $\lambda_0 d_i = 2$. a: $T/T_d = 0.05$, b: $T/T_d = 0.3$ and c: $T/T_d = 0.6$.

Fig. 7. Maximum Josephson current $J_C(\alpha, \beta, T)$ in $d/I/d$ junction with $\alpha = -\beta$ plotted as a function of temperature with $\kappa = 0.5$. A: $\alpha = 0.05\pi$, B: $\alpha = 0.1\pi$, and C: $\alpha = 0.12\pi$. a: $\lambda_0 d_i = 0$, b: $\lambda_0 d_i = 1$, and c: $\lambda_0 d_i = 3$.

Fig. 8. Positive and Negative component of $J_C(\alpha, -\alpha, T)$ obtained from curve b of Fig. 7B as a function of temperature. a: $G_p(\varphi_M)$, b: $\mid G_n(\varphi_M) \mid$, and c: $R_N J_C(\alpha, -\alpha, T)$. In the inset φ_M is plotted as a function of temperature.

Fig. 9. Josephson current $I(\varphi)$ is plotted near T_j, where jump of the φ_M occurs. a: $T = 0.125T_d$ and b: $T = 0.175T_d$. The same parameters are used as in Fig. 8.

Fig. 10. $B(\alpha, -\alpha, T)$ plotted as a function of α with $\kappa = 0.5$ for A: $\lambda_0 d_i = 1$ and B: $\lambda_0 d_i = 3$. a: $T/T_d = 0.05$, b: $T/T_d = 0.3$, c: $T/T_d = 0.6$, and d: Sigrist and Rice's result (SR theory).

Fig. 11. Maximum Josephson current in $d/I/n/I/d$ junction is plotted as a function of temperature for $\alpha = \beta = 0$. a: $L = 0.5\xi_0$ and b: $L = \xi_0$, with $\xi_0 = \hbar v_F/\Delta(0)$.

Fig. 12. Maximum Josephson current in $d/I/n/I/d$ junction is plotted as a function of temperature for $\alpha = -\beta = 0.1\pi$. a: $L = 0.5\xi_0$ and b: $L = \xi_0$ with $\xi_0 = \hbar v_F/\Delta(0)$.

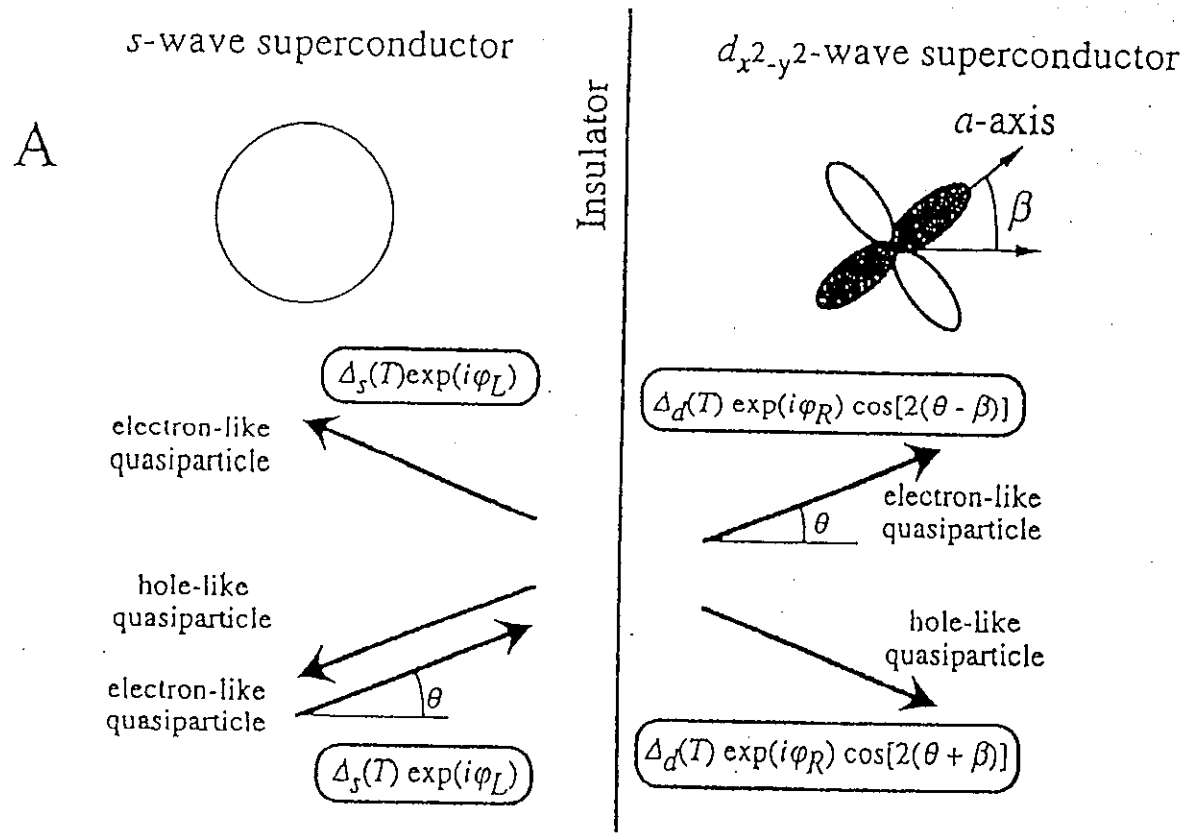
A
s-wave superconductor
Insulator
$d_{x^2-y^2}$-wave superconductor
a-axis
β
$\Delta_s(T)\exp(i\varphi_L)$
electron-like quasiparticle
$\Delta_d(T)\exp(i\varphi_R)\cos[2(\theta-\beta)]$
θ
electron-like quasiparticle
hole-like quasiparticle
electron-like quasiparticle
θ
hole-like quasiparticle
$\Delta_s(T)\exp(i\varphi_L)$
$\Delta_d(T)\exp(i\varphi_R)\cos[2(\theta+\beta)]$

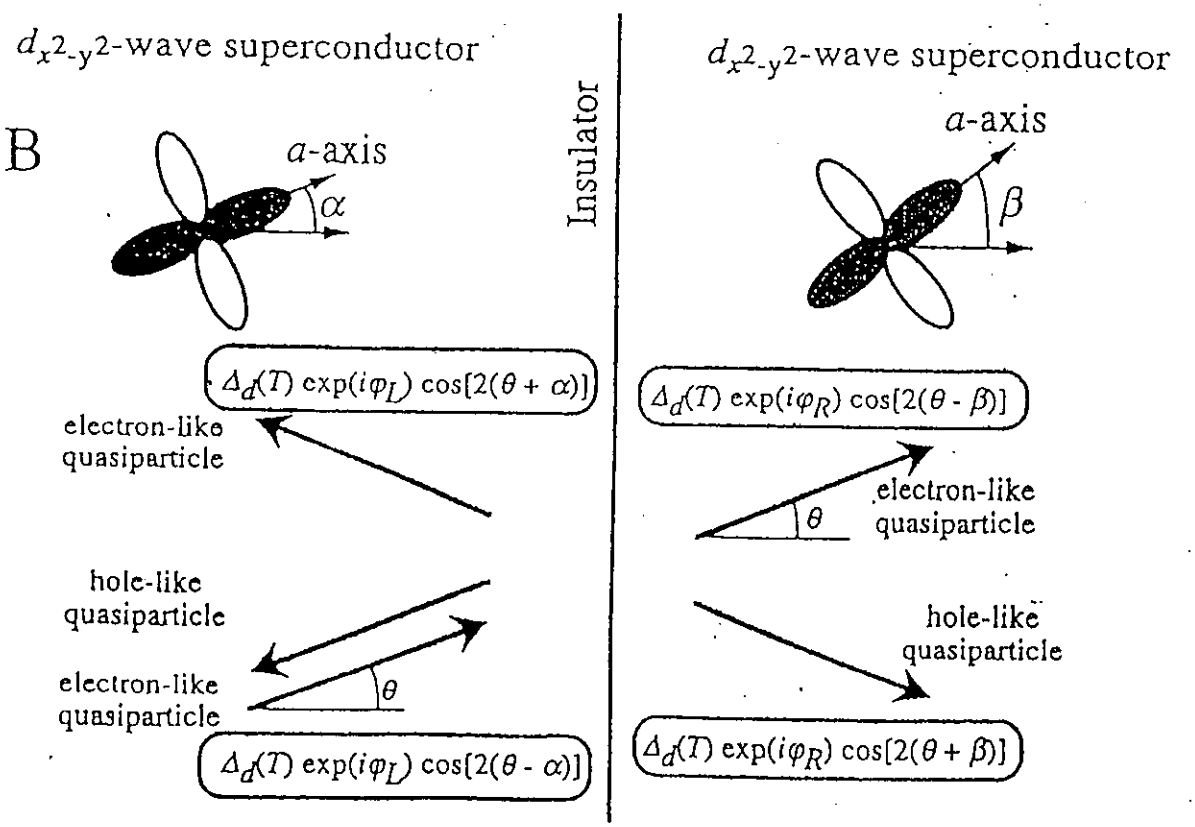
B
$d_{x^2-y^2}$-wave superconductor
Insulator
$d_{x^2-y^2}$-wave superconductor
a-axis
α
a-axis
β
$\Delta_d(T)\exp(i\varphi_L)\cos[2(\theta+\alpha)]$
electron-like quasiparticle
$\Delta_d(T)\exp(i\varphi_R)\cos[2(\theta-\beta)]$
θ
electron-like quasiparticle
hole-like quasiparticle
electron-like quasiparticle
θ
hole-like quasiparticle
$\Delta_d(T)\exp(i\varphi_L)\cos[2(\theta-\alpha)]$
$\Delta_d(T)\exp(i\varphi_R)\cos[2(\theta+\beta)]$

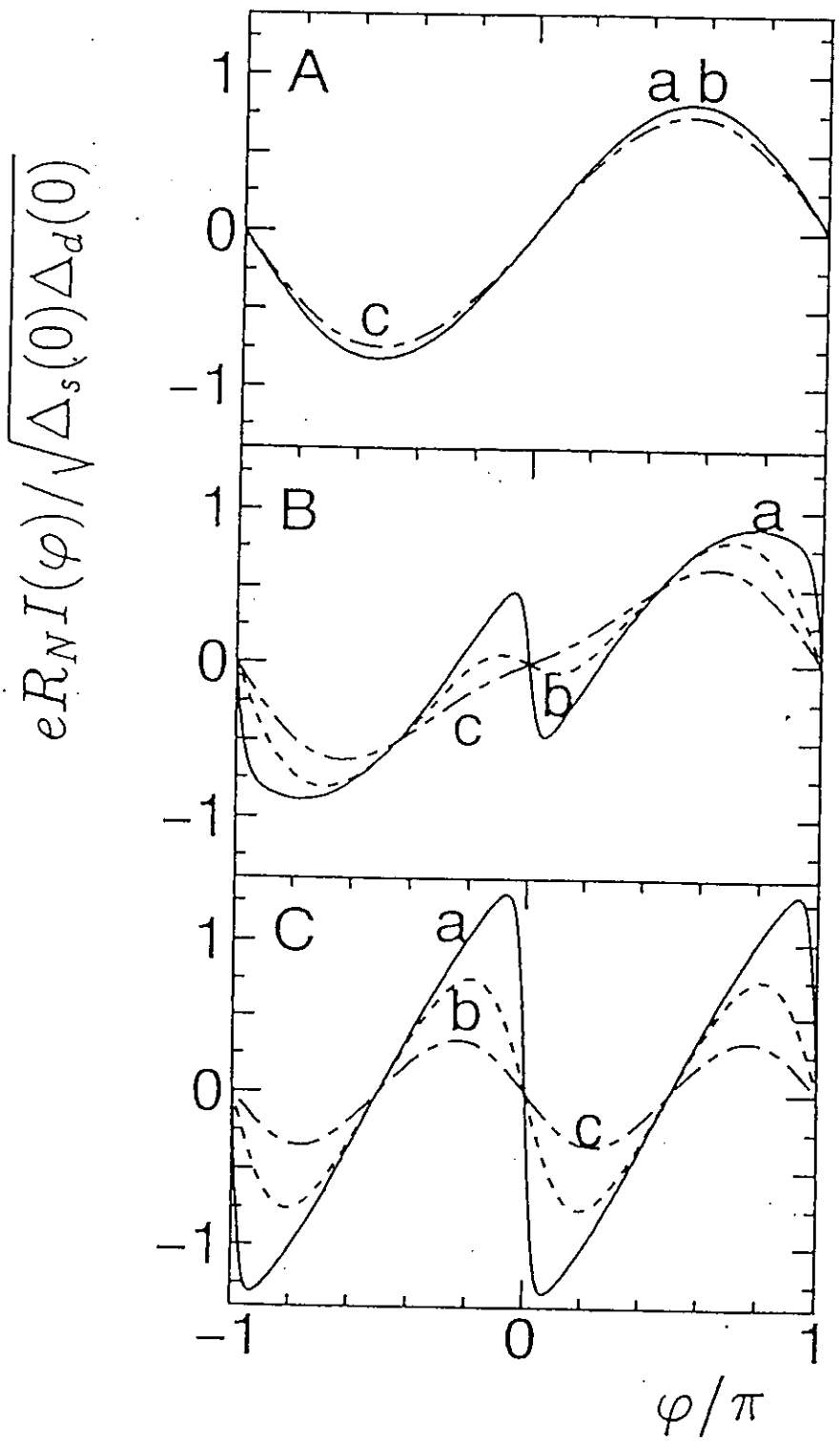
A
B
C
a
b
c
1
0
−1
$eR_N I(\varphi)/\sqrt{\Delta_s(0)\Delta_d(0)}$
φ/π

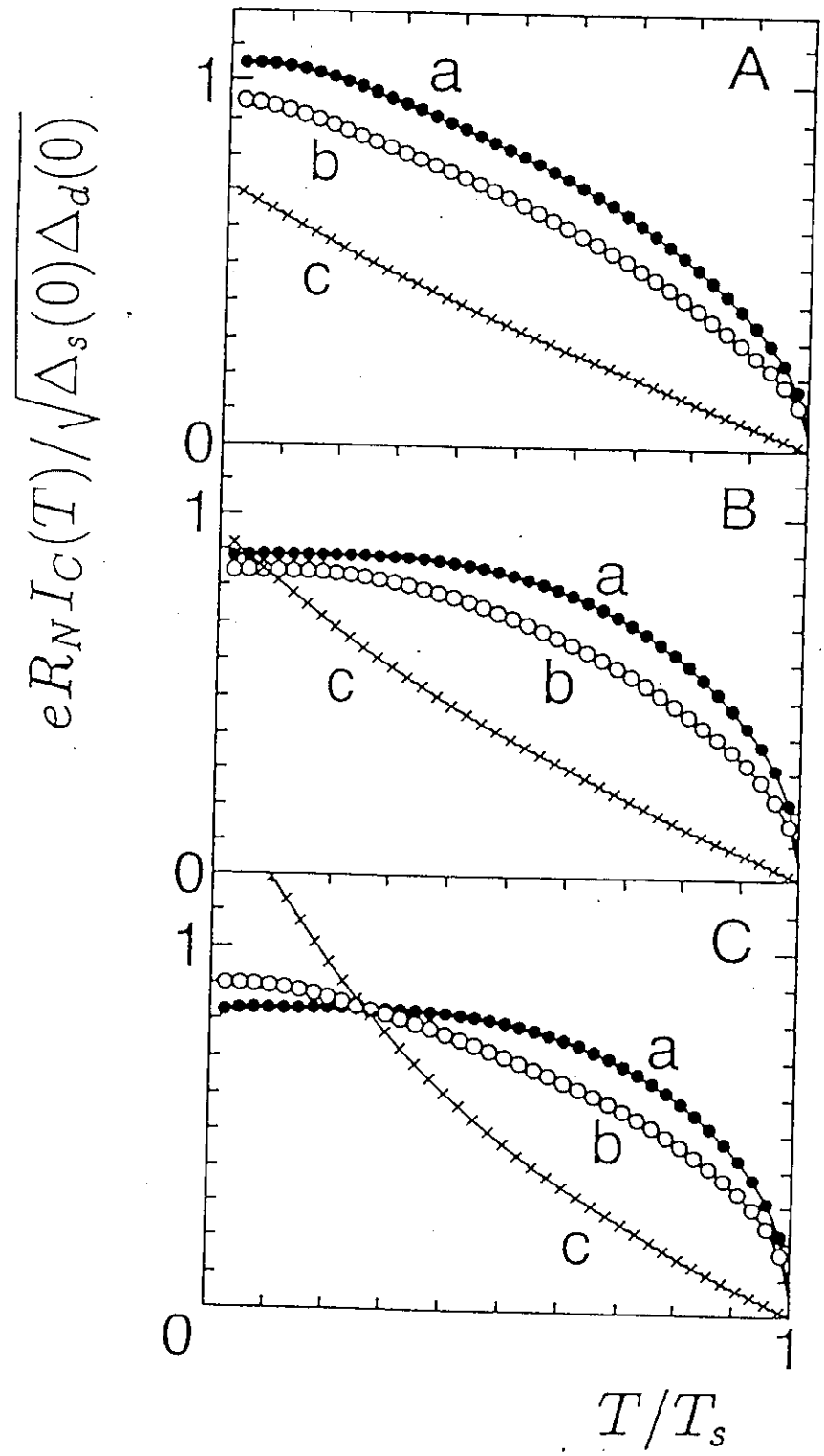
$eR_N I_C(T)/\sqrt{\Delta_s(0)\Delta_d(0)}$
1
0
A
a
b
c
B
a
b
c
C
a
b
c
0
1
T/T_s

$\alpha = \beta$

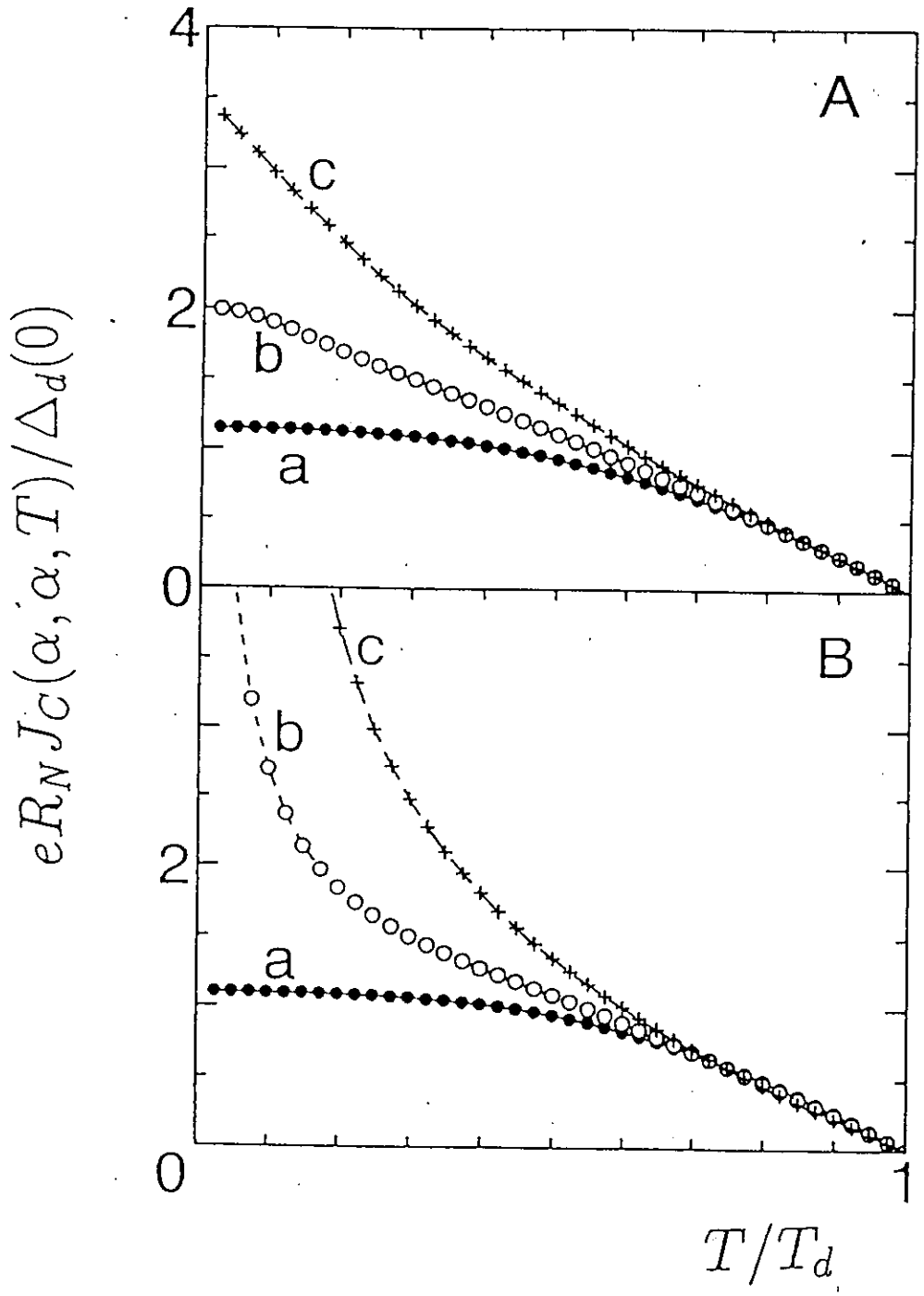

$$\alpha = \beta$$

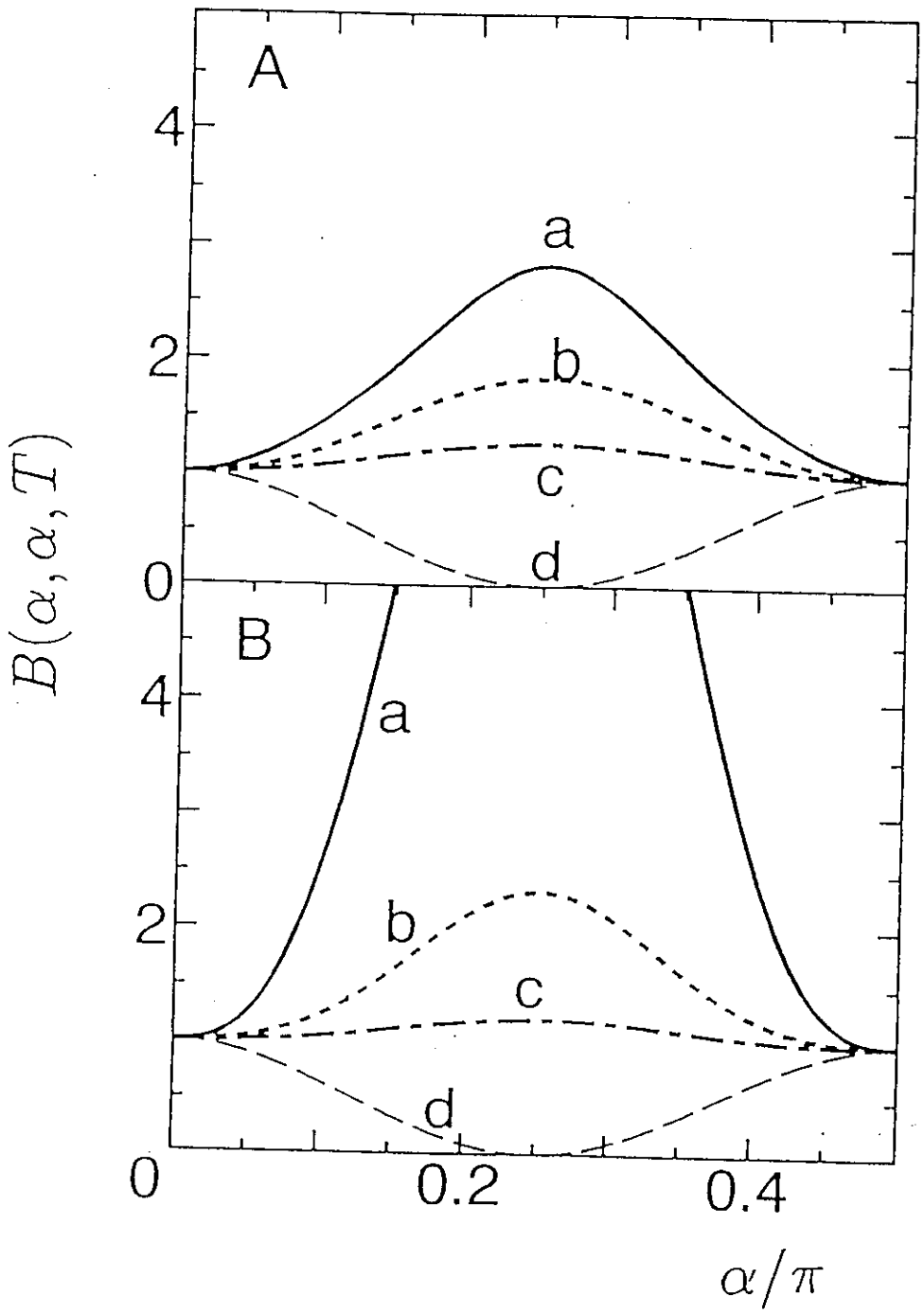

$\alpha = -\beta$

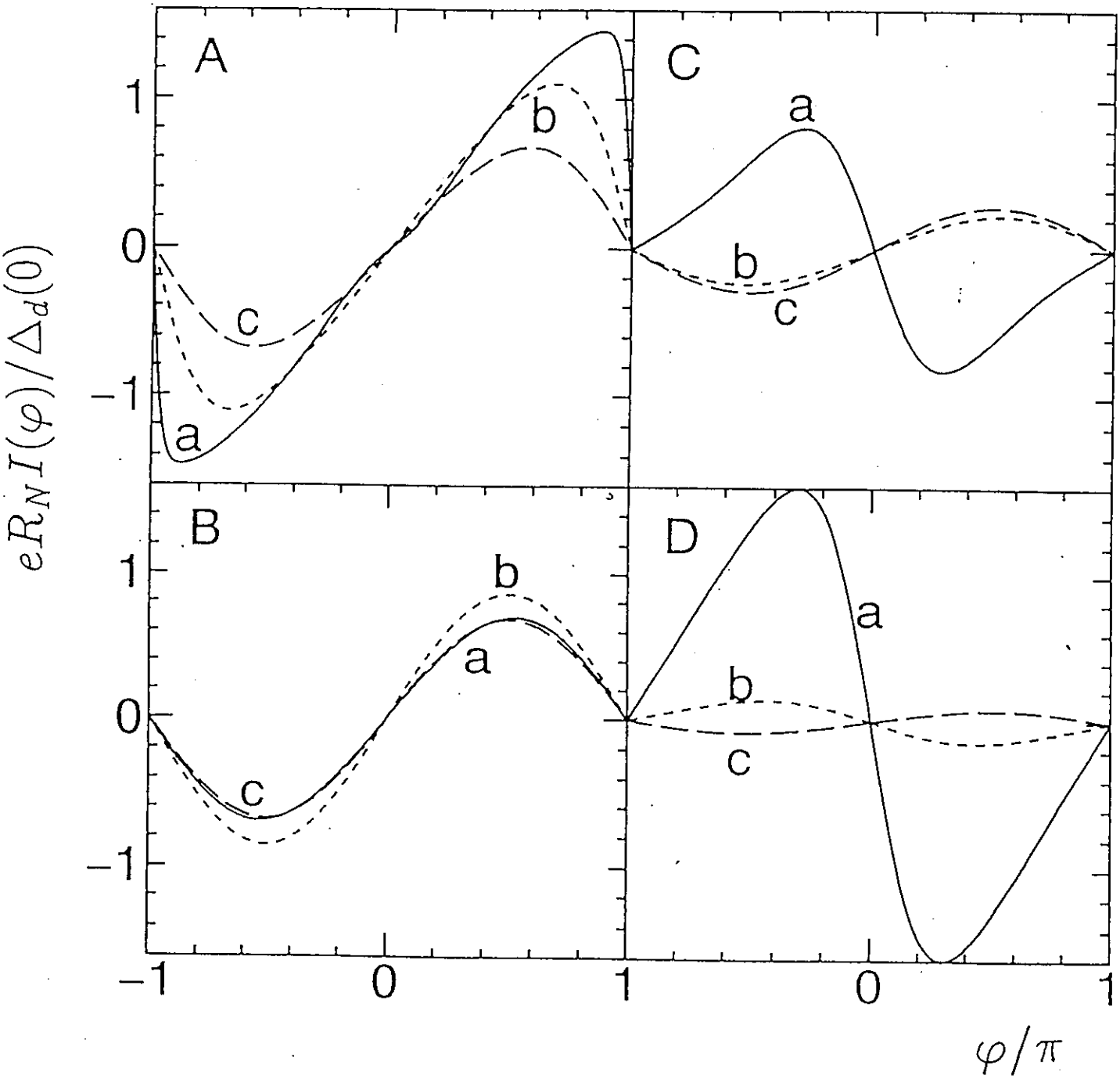

$$\alpha = -\beta$$

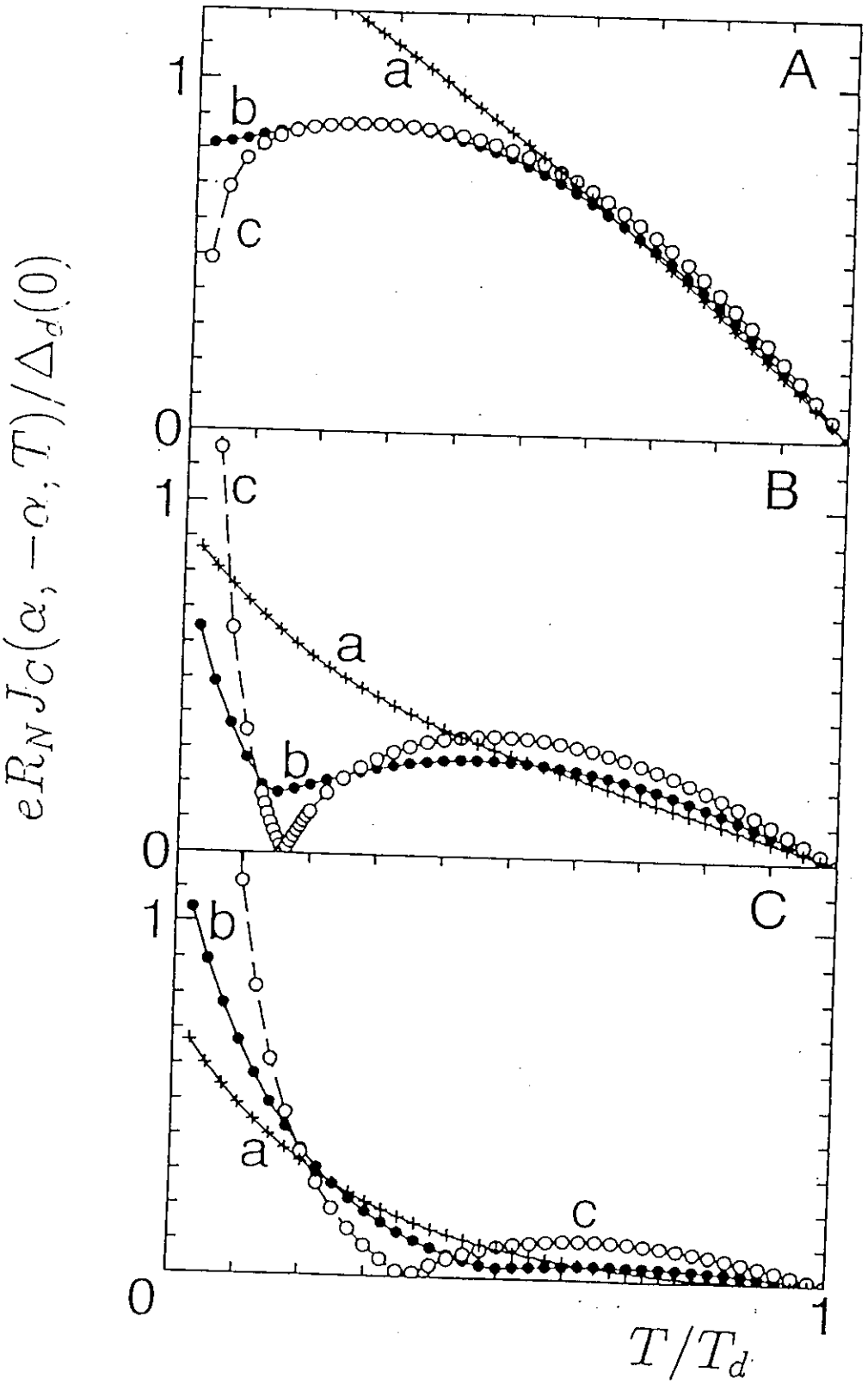

$\alpha = -\beta$

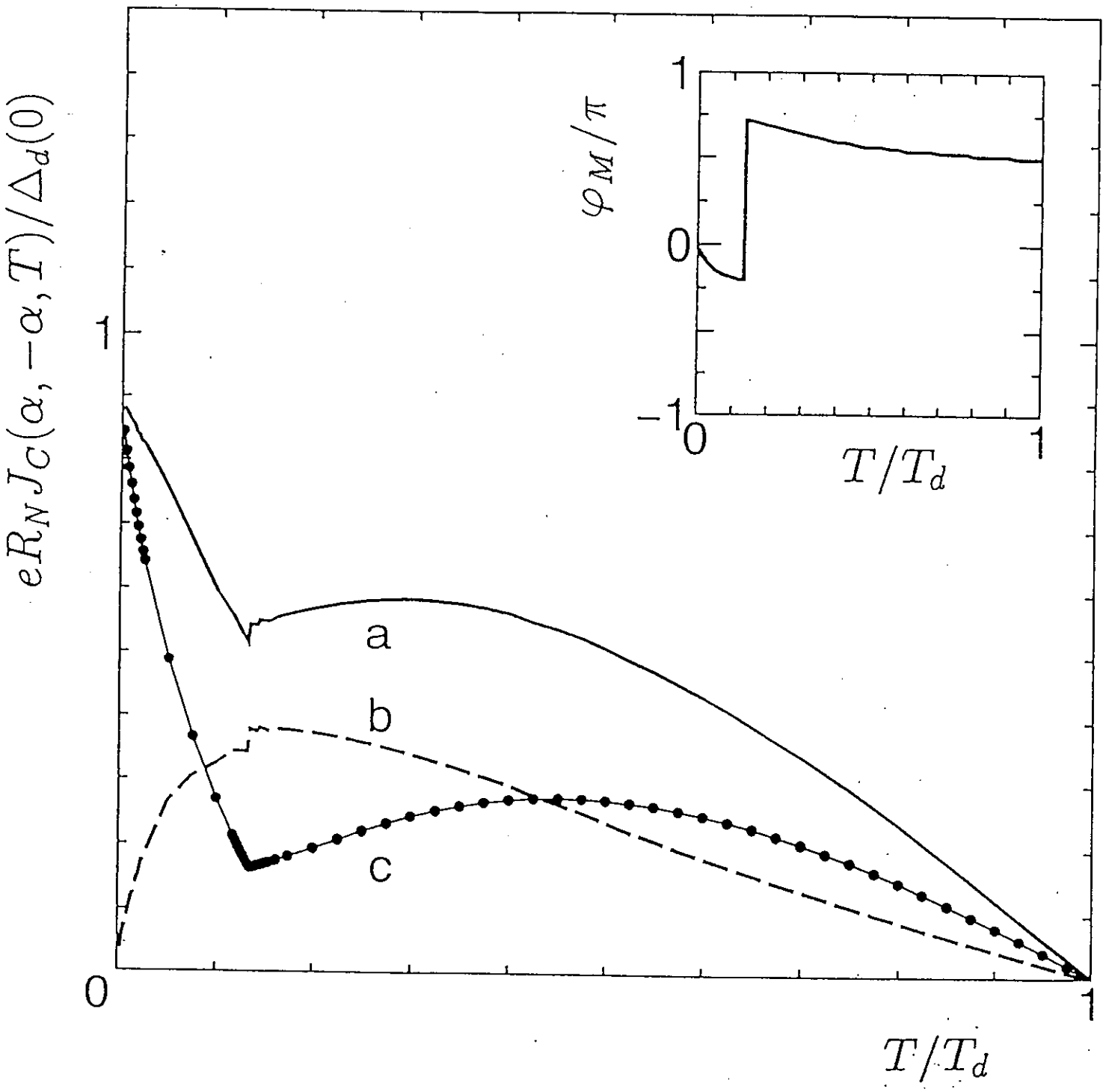

$\alpha = -\beta$

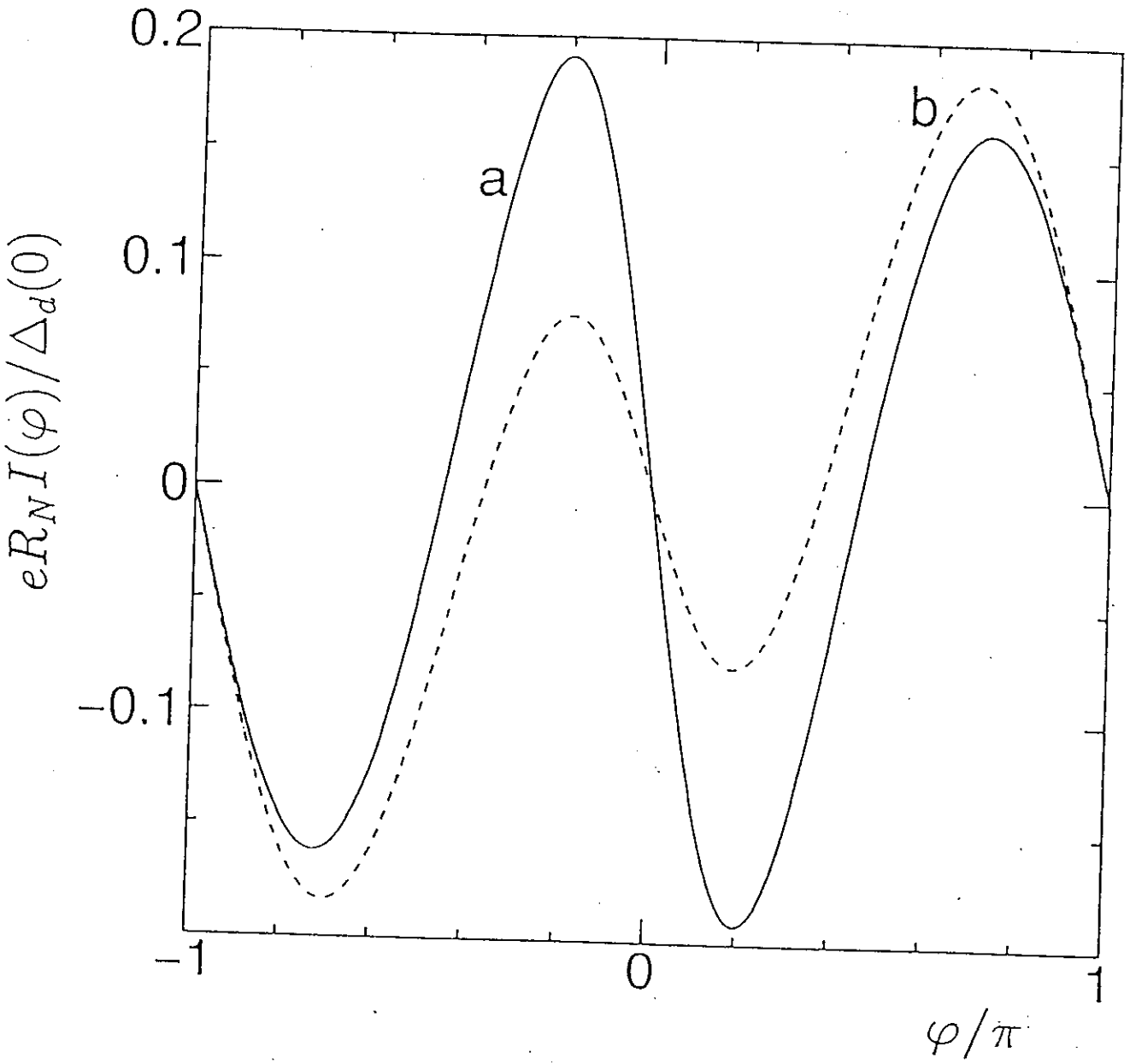

$$\alpha = -\beta$$

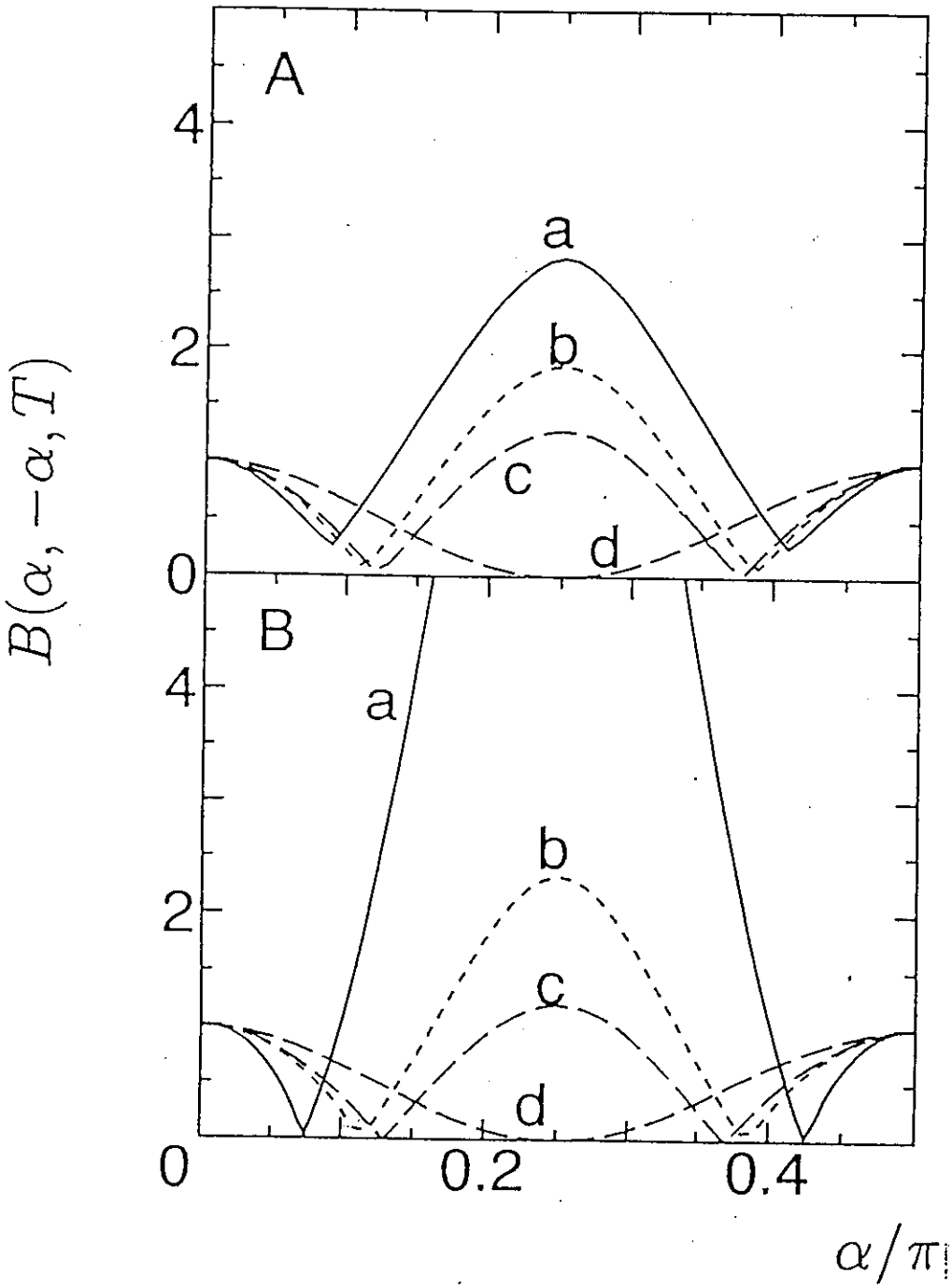

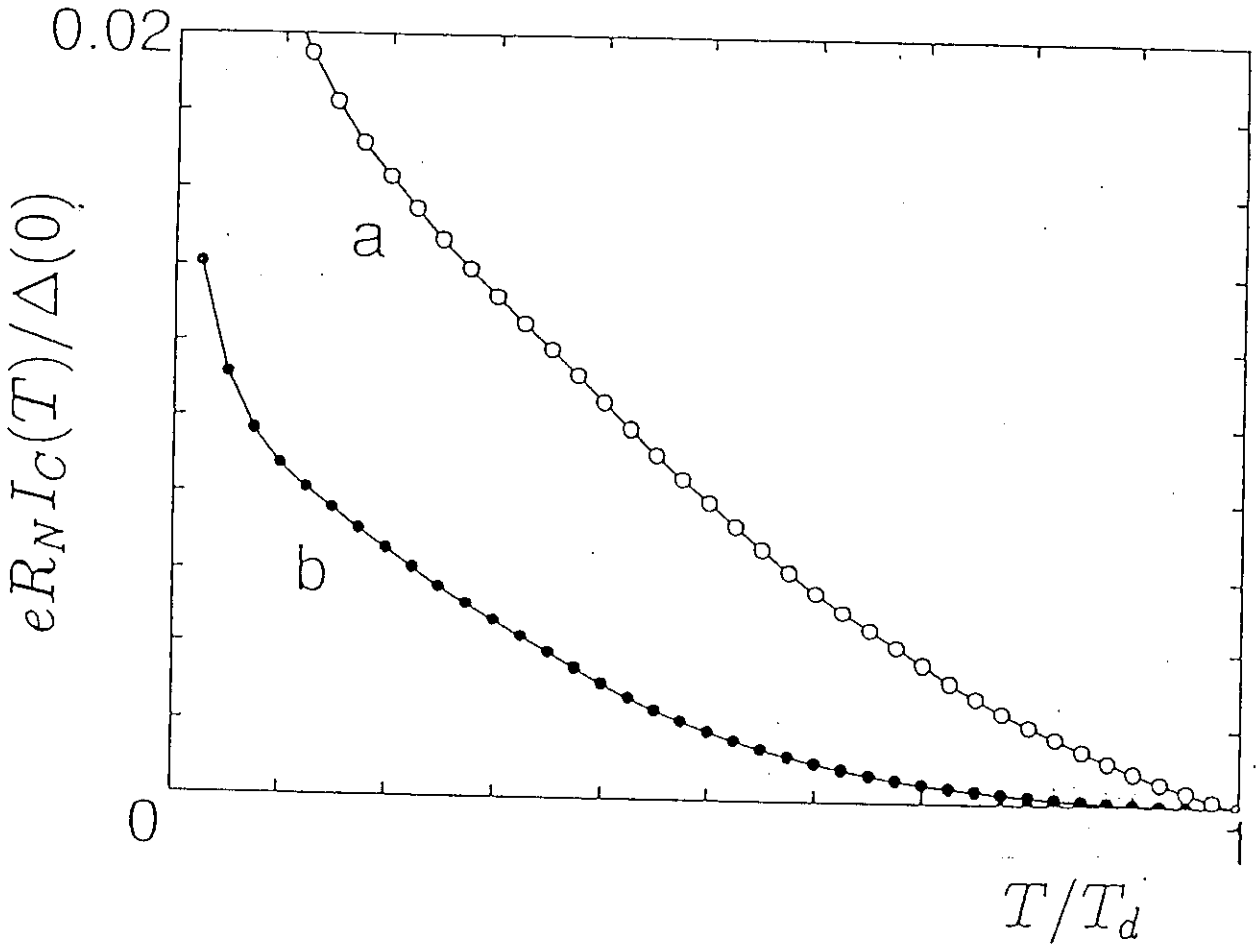
0.02
0
1
a
b
$eR_N I_C(T)/\Delta(0)$
T/T_d

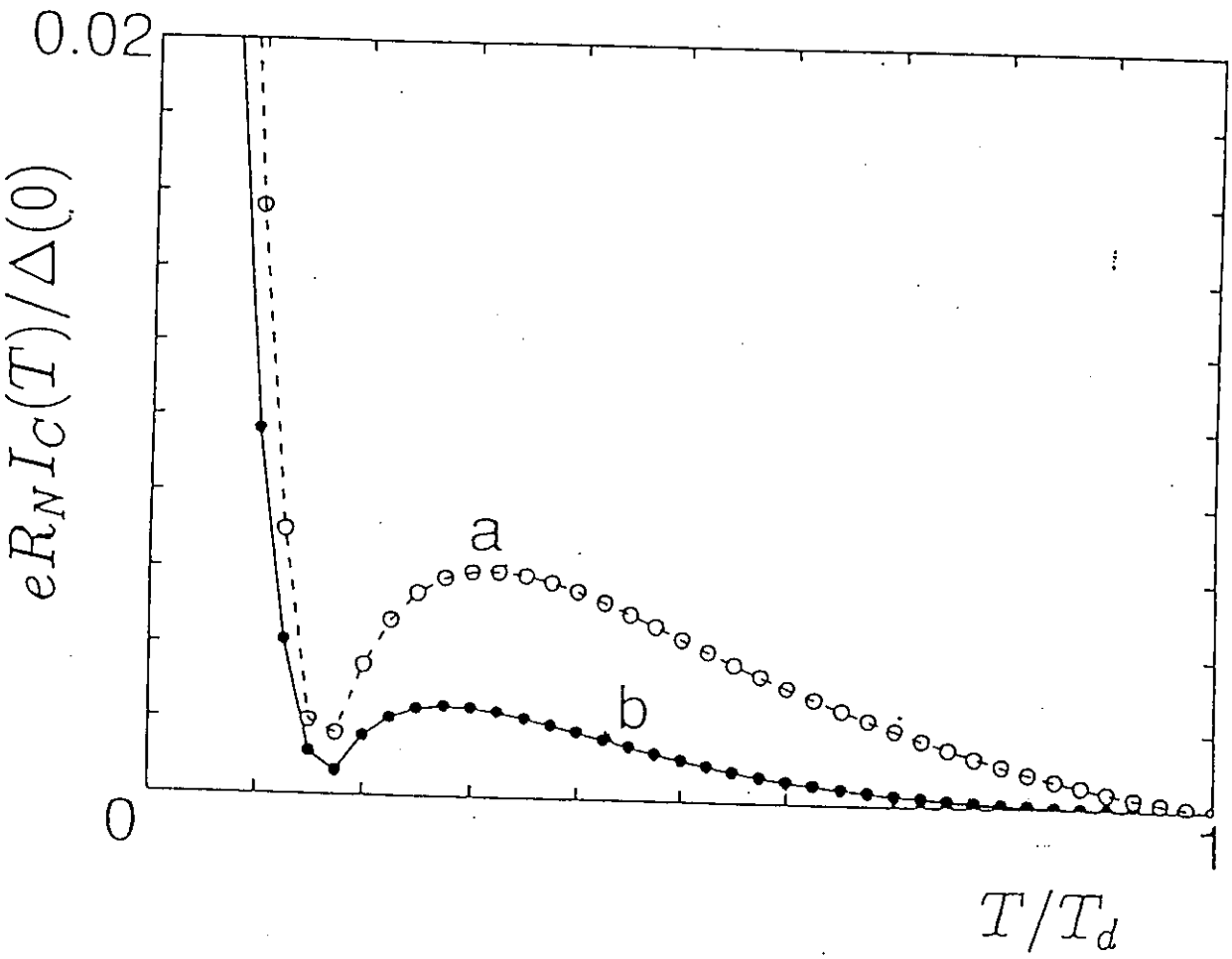
0.02
0
1
$eR_N I_C(T)/\Delta(0)$
T/T_d
a
b